

# Investigating the Impacts of a Separation Standard for UAS Operations in Enroute and Transition Airspace

Marcus Johnson<sup>1</sup>, Eric R. Mueller<sup>2</sup>, and Confesor Santiago<sup>3</sup>  
*NASA Ames Research Center, Moffett Field, CA 94035*

Unmanned aircraft systems will be required to equip with a detect and avoid system in order to satisfy the federal aviation regulations to remain well clear of other aircraft. To comply with regulations in today's operations manned aircraft must "see and avoid" other aircraft and use subjective judgment to determine whether those aircraft are well clear. For a detect-and-avoid (DAA) system to satisfy the requirement to stay well clear, a quantitative definition of well clear needs to be defined and evaluated. Definitions for the boundary of well clear have been proposed by the Unmanned Aircraft System (UAS) Executive Committee Science and Research Panel (SaRP) and the Radio Technical Commission for Aeronautics (RTCA) Special Committee 228 on Detect and Avoid Systems. This study investigates the interoperability implications of UAS using proposed well clear definitions as a separation standard for conducting operations in the national airspace system. The first analysis in the study focuses on the effect of variations in well clear definition parameters on the rate of losses of well clear per flight hour. The second analysis considers three well clear definitions and presents the relative state conditions of intruder aircraft as they encroach upon the well clear boundary. The third analysis focuses on the definition of the alerting criteria needed to inform the UAS operator of a potential loss of well clear. All three analyses are conducted in a NAS-wide fast-time simulation environment using UAS aircraft models, proposed UAS missions, and historical air defense radar data to populate the background traffic operating under visual flight rules. The results from the three analyses presented in this study inform the safety case, requirements development, and the operational environment for the DAA minimum operational performance standards.

## I. Introduction

Regulations that establish operational and performance requirements for unmanned aircraft systems (UAS) are being developed by a consortium of government, industry and academic institutions.<sup>1</sup> Those requirements will apply to the new detect-and-avoid (DAA) systems and other equipment necessary to integrate UAS with the National Airspace System (NAS) and are determined according to their contribution to the overall safety case for such an integration. Several key gaps must be closed in order to link equipment requirements to an airspace safety case. Foremost among these is calculation of the degree to which a particular system mitigates violation of an aircraft separation standard, which is known as the system's "risk ratio."<sup>VI</sup> The risk ratio of a DAA system, in combination with risk ratios of other collision mitigation mechanisms, will determine the overall safety of the airspace measured in terms of the number of mid-air collisions per flight hour. The second gap is the lack of a definition of a separation standard that the DAA system is intended to maintain,<sup>VI</sup> without which a risk ratio cannot be calculated. A third gap is the alerting criteria needed for a UAS operator gain situation awareness and remain well clear of other aircraft. Defining and evaluating the risk ratios as a function of the DAA system parameters, the UAS separation standard, and the alerting criteria requires a simulation capability that incorporates aerodynamic performance and mission characteristics of future UAS operations. Together, the UAS characteristics and DAA separation standard will allow determination of the frequency and types of encounters expected between UAS and manned aircraft that are necessary to calculate the risk ratio, develop the safety case, and develop the performance requirements of the DAA system.

Previous research investigating aircraft encounter rates and characteristics and the safety of new collision mitigation methods has largely been focused on the existing airspace and aircraft using existing separation standards. This research established the risk ratio metric as a valid method of demonstrating that a safety standard

<sup>1</sup> Aerospace Engineer, Aviation Systems Division, MS 210-10; [marcus.johnson@nasa.gov](mailto:marcus.johnson@nasa.gov), Member, AIAA

<sup>2</sup> Aerospace Engineer, Aviation Systems Division, MS 210-10; [eric.mueller@nasa.gov](mailto:eric.mueller@nasa.gov), Senior Member, AIAA

<sup>3</sup> Aerospace Engineer, Aviation Systems Division, MS 210-10; [confesor.santiago@nasa.gov](mailto:confesor.santiago@nasa.gov), Member, AIAA

had been met.<sup>II</sup> Standards for collision avoidance systems (e.g. TCAS) and air traffic control (ATC)-provided separation were based on the performance of existing transponder and radar systems, respectively, along with human performance. Separation standards for DAA systems cannot be determined in the same way because there are not yet any operational or performance requirements for such systems, so more recent approaches have focused on an acceptable risk of collision without a DAA system.<sup>X</sup> The UAS Executive Committee Science and Research Panel (SaRP) evaluated three candidate separation standards, however these definitions have not yet been converted into resulting risk ratios.<sup>VI</sup> Aircraft mission and aerodynamic performance parameters that are central to calculating risk ratios have also been based on existing airspace operations;<sup>V</sup> they do not incorporate a wide range of new UAS aircraft performance and mission characteristics.<sup>VI</sup> These characteristics are necessary because most manned aircraft in enroute and transition airspace fly from origin to destination along fixed airways, while many unmanned aircraft need to perform “mission-oriented” operations (e.g. flying a loitering pattern, grid pattern, or non-predetermined missions with frequently changing flight plans). This difference in mission profiles may create different conflict situations between unmanned and manned aircraft.<sup>II</sup> Several studies have investigated the airspace impact of a single UAS mission in northern California, but these analyses have not been extended to other geographic areas or included other UAS aircraft types or missions.<sup>XVII,III</sup> The key to demonstrating the requirements for safely integrating UAS with the NAS will be to extend such analyses to a representative set of UAS types and missions over a broad geographic area using candidate separation standards so that a collision mitigation risk ratio for DAA systems may be calculated.

The original contribution of the research reported in this paper is the denominator of the DAA risk ratio: the rate at which the DAA separation standard is violated given no collision mitigation methods are employed. This violation rate is provided as a function of the parameters of four different metrics for defining the separation standard, which will provide regulators tasked with selecting a single standard an understanding of how their selection may affect the predicted aircraft collision rate. The sensitivity of the violation rate will also assist DAA system designers in selecting buffers around the separation standard that reduce the probability of violation without disrupting surrounding traffic. The simulations used to collect these statistics considered thousands of UAS flight plans and tens of thousands of UAS flight hours in many geographic areas so that the results would be broadly representative of domestic U.S. operations, allowing presentation of the metrics as a function of altitude and season. A secondary product of the analysis of encounter rates is determination of the relative states between encountering aircraft when the separation standard is violated. This information may be used to determine surveillance system requirements, establish initial conditions in Monte Carlo aircraft interaction simulations, provide guidelines for the design of DAA traffic displays for UAS pilots, and indicate the interoperability between the DAA separation standard and existing separation standards. A third contribution of this work considers the impact of the alerting logic on the UAS operator’s ability to maintain well clear of other aircraft. In particular, the timeliness, frequency, and reliability of the alerts presented to the operator are evaluated. This information can be used to inform the DAA sensor requirements, which have a large contribution to the risk ratio calculation and the safety case. The results presented in this paper represent an essential contribution to the calculation of the DAA risk ratio and therefore an important step in the design of systems and procedures that will support safe integration of UAS with the NAS.

The rest of the paper is organized as follows: Section II introduces the well clear definitions and alerting logic used in subsequent analyses; Section III outlines the three analysis methodologies; Section IV details the simulation methodology including the simulation platform, UAS models, traffic scenarios, mission description and mission implementation; Section V presents the results of the three analyses; and Section VI provides the concluding remarks. The first analysis presented in this paper evaluates the effect of the well clear definition parameters on the rate of losses of well clear. The second analysis instantiates three well clear definitions and evaluates the relative state information when there is a loss of well clear. The third analysis focuses on the alerting criteria and the characteristics at the instance of first alert.

## **II. Definitions for Well Clear Analysis**

The FAA-sponsored Sense-and-Avoid (SAA) Workshop<sup>I</sup> defines SAA as “the capability of a UAS to remain well clear from, and avoid collisions with, other airborne traffic. SAA provides the intended functions of self separation and collision avoidance compatible with expected behavior of aircraft operating in the NAS.” The self-separation (SS) function of an SAA system is intended as a means of compliance with the regulatory requirements (14CFR Part 91, §91.111 and §91.113) to “see and avoid” and to remain “well clear” of other aircraft. Since the publication of that workshop report, the UAS community has shifted to using the term “detect and avoid” rather than “sense and avoid,” a distinction without a difference. This paper will use DAA for consistency.

The concept of well clear has been proposed as an airborne separation standard to which a DAA system must adhere,<sup>VI</sup> and performing SS correctly means remaining well clear of other aircraft. The well clear definition is a separation standard used by the SS function to determine what action is necessary to remain an appropriate distance from other aircraft. The standard will require a UAS be able to detect and avoid other aircraft in sufficient time as to avoid creating a collision hazard. The time or distance thresholds defining a loss of well clear could be unique for each intruder based on closure rate, performance characteristics, encounter geometry, and other variables. Therefore, it is necessary to define an explicit and quantitative definition of well clear so that the contribution of the SS function to the overall safety for a given airspace can be unambiguously determined.

The second SAA workshop<sup>IV</sup> defines “well clear” as the state of maintaining a safe distance from other aircraft that would not normally cause the initiation of a collision avoidance(CA) maneuver by either aircraft. The following DAA implementation principles could also be utilized to define the well clear standard:<sup>V</sup>

- Separation should be large enough to avoid corrective maneuvers from intruders (e.g., resolution advisories for TCAS-equipped intruders), to minimize traffic alert issuances by controllers, and to avoid excessive concern for proximate see-and-avoid pilots;
- Deviations should be small enough to avoid disruptions to traffic flow and vary appropriately with encounter geometry and operational areas (e.g. terminal, transition, enroute).

Ongoing research efforts are identifying quantifications for these DAA interoperability criteria; however assessing the overall impact to the NAS is still an open research area. This paper aims to address the impact on the NAS due to quantification of these criteria by determining how frequently aircraft operating in class E airspace and transiting to class A airspace encounter each other as a function of the well clear boundary definition and the nature of the UAS mission profiles. The proposed definitions are taken from a recent FAA report,<sup>VI</sup> a dedicated US Government workshop on well clear,<sup>VI</sup> and variations on methods used by TCAS II.<sup>VII</sup>

A metric originally used in the Traffic Alert and Collision Avoidance System (TCAS) collision detection logic<sup>VII</sup> to estimate the time to closest point of approach between two aircraft is based on the concept of “tau,” which is calculated as the ratio of slant range between aircraft to their range rate and measured in seconds:

$$\tau = -\frac{r}{\dot{r}} \quad (1)$$

The TCAS detection logic also includes a vertical metric that approximates the time until both aircraft will be at co-altitude. This metric is referred to as vertical tau and is calculated as the ratio of the difference in altitude to the vertical range rate and measured in seconds:

$$\tau_{vert} = -\frac{\Delta h}{\Delta \dot{h}} \quad (2)$$

Note that a tau value is positive when the UAS and the intruder are on converging paths and negative when they are on diverging paths. Tau represents an approximation of the time to closest point of approach (CPA). The CPA is defined as the minimum slant range between aircraft pairs, and in the case of a direct collision course (separation at the CPA is zero) the tau computation is equal to time to CPA. If the aircraft are not on a collision course, then tau is only an approximation of time to CPA. In this case, the CPA serves as an asymptote to the tau metric (since  $\dot{r} = 0$  at CPA), and therefore the minimum value of tau will occur just prior to the CPA. Since the ratio of range to range rate will generally be lower with closer points of approach, this minimum value of tau approximates the severity of the encounter. This property of tau means that selection of a minimum tau value at which to alert for a loss of well clear determines not only the *time* to react to the threat, but also the size of protected airspace within which a given threat encounter will cause an alert. When an intruder aircraft is predicted to create an encounter with a tau value below the minimum, the DAA system may trigger an alert to an imminent loss of well clear.

One issue with the tau metric occurs for encounters where the rate of closure is very low, as described in the TCAS II Manual.<sup>VII</sup> For these encounters the calculated tau may be large while the physical separation may be quite small. In such a situation, the calculated tau value no longer assures adequate separation because a sudden acceleration that increases the closure rate (e.g., a turn) would not give sufficient alerting time to avoid a loss of well clear or even a near mid-air collision (NMAC). An NMAC is defined by an aircraft pair coming within proximity of less than 500 ft radial horizontal and 100 ft vertical separation from each other. To provide protection in these types of encounters, a modified alerting threshold, often referred to as “modified tau,” is used by TCAS II.<sup>VII,VIII</sup> This metric uses a new parameter, “distance modification” (DMOD), to provide a minimum range at which to alert regardless of the calculated value of tau. Modified tau is computed as

$$\tau_{mod} = \begin{cases} -\frac{(r^2 - DMOD^2)}{r\dot{r}} & \text{for } r \geq DMOD \\ 0 & \text{for } r < DMOD \end{cases}, \quad (3)$$

where the distance modification represents a threat boundary encircling the ownship aircraft that triggers an alert when the boundary is violated. The value(s) of the constant DMOD used for a well-clear separation standard is an

independent variable in the well-clear definition. For the purposes of this study, three sets of DMOD constants will be investigated to gauge the sensitivity of losses of well clear to this parameter. The modified tau metric was introduced to address the slow-rate-of-closure scenarios that caused a safety hazard not identified by the tau metric, however modified tau also has limitations. For situations in which aircraft are on converging paths with a high rate of closure and a large miss distance, the modified tau metric will indicate an alert is required. This type of alert would be considered a “nuisance” to the UAS operator, as the system could alert even when the miss distance is much larger than DMOD. To illustrate this scenario, consider two aircraft on converging paths traveling on opposite headings at 600 knots and horizontally offset by 5.9 nmi. In this scenario, the minimum modified tau measurement would be at 35 seconds, which hypothetically could be below an alerting threshold instructing the pilot to initiate a collision avoidance maneuver. However these aircraft are separated by 5.9 nmi at CPA which is greater than the enroute radar separation used by air traffic controllers. TCAS II addresses this limitation in the tau and modified tau measures by applying a horizontal miss distance (HMD) filter at CPA. This filter removes alerts for encounters in which separation at CPA is greater than the HMD parameter.<sup>V</sup>

The first definition presented in this work considers the minimum protected airspace between pairs of aircraft in order to establish a relationship between the time-based modified tau parameter and the rate of encounters experienced between UAS and VFR aircraft for a range of time thresholds. It considers the time threshold as an independent variable. The second definition considers three candidate well clear definitions and investigates the rates of losses of well clear for those given definitions. The third definition considers the alerting threshold and the state information of the intruder relative to the ownship at the instant the system alerts the pilot to a threat.

#### A. Definition 1: Minimum Airspace Separation

This definition considers the minimum airspace separation between pairs of aircraft using the modified tau and time to co-altitude with a horizontal miss distance at CPA metrics to define the volume of the airspace between the UAS ownship and intruder aircraft. Consider the time history of a given pair of aircraft on converging paths and compute a separation metric associated with modified tau and time to co-altitude given as

$$J_1 = \begin{cases} \tau_{mod}^2 + \tau_{vert}^2 & \text{where } \{ \tau_{mod} \geq 0, \tau_{vert} \geq 0, r_{xy}(t_{CPA}) \leq HMD^*, \Delta h \leq ZTHR \} \\ \infty & \text{else} \end{cases}, \quad (4)$$

where  $HMD^*$  is the horizontal miss distance threshold,  $ZTHR$  is the vertical separation threshold,  $\Delta h$  is the current vertical separation,  $r_{xy}(t_{CPA})$  is the predicted horizontal miss distance at CPA, and  $\tau_{mod}, \tau_{vert}$  denote the modified tau and time to co-altitude calculations given by equations (2) and (3), respectively. The larger the value of the separation metric  $J_1$ , the more airspace is separating the UAS ownship and the intruder aircraft. Definition 1 is defined as the couple  $\{\tau_{mod}, \tau_{vert}\}$  such that the cost in (4) is minimized. This couple indicates the point at which the minimum separation exists between the aircraft pair with respect to time and space. This study considers several configurations of Definition 1 in the subsequent analysis. One such configuration (D1.1) corresponds to the TCAS II values for DMOD, ZTHR, and HMD for Class E airspace between 10,000-20,000 ft. The other configurations are effectively perturbations of the DMOD, ZTHR and HMD parameters of D1.1. Each definition configuration is detailed in Table 1.

Configuration	DMOD [nmi]	ZTHR [ft]	HMD [ft]
D1.1	0.80	600	4861
D1.2	0.80	450	4861
D1.3	0.80	800	4861
D1.4	0.55	600	3342
D1.5	1.10	600	4861
D1.6	0.55	600	3342
D1.7	1.20	600	7292
D1.8	0.80	600	4000
D1.9	0.80	475	6000

**Table 1: Minimum Airspace Separation Configuration Parameters.**

#### B. Definition 2: Well Clear Boundary

The remaining definitions differ from Definition 1 by fixing the threshold values rather than considering them as independent variables. The remaining definitions are considered qualitative definitions of well clear as a separation standard. These definitions will be used to determine whether one aircraft has violated the well clear boundary of another aircraft. Definition 2 is the most similar to the detection logic in TCAS II and consists of a set of criteria

based on the time to co-altitude and modified tau definitions. This definition consists of temporal and distance-based criteria in the horizontal dimension as

$$\text{Criterion 1: } 0 \leq \tau_{mod} \leq \tau_{mod}^* \text{ AND } r_{xy}(t_{CPA}) \leq HMD^* , \quad (7)$$

and criteria in the vertical dimension as

$$\text{Criterion 2: } 0 \leq \tau_{vert} \leq \tau_{vert}^* \text{ OR } |\Delta h| \leq ZTHR , \quad (8)$$

where  $\tau_{vert}^*$  and  $\tau_{mod}^*$  are the time to co-altitude and tau thresholds, respectively. From (7) and (8), a loss of well clear (LOWC) is defined as

$$\text{LOWC: Criterion 1 is true AND Criterion 2 is true.} \quad (9)$$

This study considers two configurations for this definition based on the investigation of well clear definitions proposed by the SaRP. The SaRP chose three well clear definitions, tuning parameter values in each definition to meet a common threshold of 1.5% for unmitigated near mid-air collision (NMAC) risk using MIT Lincoln Lab's Uncorrelated Encounter Model.<sup>ix</sup> The parameters of two such well clear definitions are detailed in Table 2, while the third well clear definition proposed by the SaRP is not presented in this work. The third definition that is considered in this study (D2.3) has the same parameters as D2.2, however the altitude separation threshold, denoted as ZTHR, is less than the distance that air traffic controllers would consider as operationally acceptable separation with VFR traffic (500 ft).

Configuration	$\tau_{mod}^*$ [sec]	$\tau_{vert}^*$ [sec]	DMOD [nmi]	ZTHR [ft]	HMD [ft]
D2.1	30	20	0.987	475	6000
D2.2	35	0	0.658	700	4000
D2.3	35	0	0.658	450	4000

**Table 2: Well Clear Boundary Configuration Parameters.**

### C. Definition 3: Alerting Threshold

The prior definitions are primarily focused on quantifying well clear and gauging the sensitivity to parameter variations within the well clear definition. Another important factor in safe operations is the pilot's ability to gain situation awareness of a conflict and have sufficient time to avoid violating the quantified well clear protected airspace between the UAS and an intruding aircraft. Definition 3 considers the temporal threshold, referred to as the self-separation threshold (SST), at which the DAA system should alert the pilot of an imminent threat. The definition is the same as the definition given by Criteria 1 and 2 in (7) and (8), respectively. The parameters that are considered for the modified tau alerting threshold definition are detailed in Table 3.

Configuration	SST: $\tau_{mod}^*$ [sec]	$\tau_{vert}^*$ [sec]	DMOD [nmi]	ZTHR [ft]	HMD [ft]
D3.1	90	0	0.658	450	4000
D3.2	90	0	0.658	700	4000
D3.3	110	0	0.658	700	4000
D3.4	70	0	0.658	700	4000
D3.5	90	0	0.987	700	6000
D3.6	90	0	0.9875	900	6000

**Table 3: Alerting Threshold Configuration Parameters.**

## III. Analyses of Well Clear Definitions

Three analyses of well clear definitions and alerting criteria are considered in this study. This study focuses on encounters between UAS and aircraft operating under visual flight rules (VFR) carrying a transponder that uses the 1200 Mode A transponder code (referred to as cooperative VFR aircraft). Future work will consider encounters with aircraft that are not equipped with a transponder (referred to as non-cooperative VFR aircraft).

### Analysis 1: Evaluating the effect of well clear definitions on the rate of loss of well clear.

In this analysis, the frequency of losses of well clear between UAS and manned VFR aircraft are measured as a function of the parameters defining a loss of well clear, including tau, DMOD, miss-distance filters, and vertical separation thresholds. This analysis investigates the rate of losses of well clear when a DAA mitigation is not present.

### Analysis 2: Characterizing encounters at the well clear boundaries.

This analysis focuses on the characteristics of UAS encounters with manned cooperative VFR aircraft, including range rates, relative heading and separation, and percentage of maneuvering intruders at the well clear boundary. The objective of this analysis is to study the relative time and distance separations between aircraft at the boundary of a well clear definition.

### **Analysis 3: Evaluating the alerting threshold definition and alerting criteria.**

This analysis considers criteria for alerting the UAS operator that action is necessary to avoid a loss of well clear. The parameters of each definition are varied and the analysis focuses on the relative state information at the first alert. In particular the range rates, relative heading and separation are of interest, as well as the percentage of alerts that do not result in a loss of well clear. This analysis informs the minimum sensor range required based on alerting criteria, as well as the rate of nuisance alerts due to buffers on the well-clear boundary.

## **IV. Methodology**

### **A. Simulation Platform**

The Airspace Concept Evaluation System (ACES) is a National Airspace System (NAS)-wide fast-time simulation tool.<sup>X</sup> The ACES platform models and simulates the NAS using interacting agents representing center control, terminal flow management, airports, individual flights, and other NAS elements. These agents pass messages between one another to model real-world information flows. This distributed agent-based system is designed to emulate the highly interconnected nature of the NAS, making it a suitable tool to evaluate current and envisioned airspace concepts. The approach of this study is to use ACES to investigate the effects of well clear definitions for UAS DAA systems in enroute and transition airspace. The ACES platform provides a large set of four-degree-of-freedom (4 DOF) aircraft models, including many models that mimic the flight characteristics of UAS aircraft (such as Global Hawk, Reaper, Shadow, etc.), as discussed in Section IV.B. below.

One of the inputs to ACES is the flight demand set, which consists of all of the flights to be simulated with their aircraft type, their departure and arrival airports, their departure times and their flight plans. In this study, UAS mission flight demand sets are used as inputs to the ACES platform, as well as VFR aircraft. The VFR aircraft flight data sets are synthesized from air defense radar data.

### **B. UAS Aircraft Models**

The aircraft models used in this study are derived using performance data from the Base of Aircraft Data (BADA) models. The BADA models were generated from industry data<sup>XI</sup> and validated by Intelligent Automation Inc. (IAI).<sup>XII</sup> The performance specifications required to conduct given UAS missions are detailed in Table 4, along with representative aircraft types whose performance would at least meet that which is required for the particular mission.

Mission	Aircraft	Cruise Altitude [ft]	Cruise Speed [kts]	Flight Count	Flight Duration	Total Flight Hours
Cargo Transport	Cessna 208 Caravan (C208)	2,000-16,000 MSL	146-308	1,400	20-200 min.	1887
On Demand Air Taxi	Cessna Citation Mustang (C510)	10,000-33,000 MSL	156-340	3,180	20-45 min.	1016
On Demand Air Taxi	Cirrus (SR22T)	6,000-11,000 MSL	153-166	8,720	20-45 min.	5533
Strategic Fire Monitoring	Reaper (MQ-9)	31,000 MSL	209	324	20 hrs.	5172
Tactical Fire Monitoring	Shadow (RQ7B)	3,000 AGL	72-80	2,496	1-1.5 hrs.	3164
Atmospheric Sampling	Global Hawk (RQ4A)	5,000-35,000 AGL	151-343	2,401	1.5-13 hrs.	6261
Air Quality Monitoring	Shadow (RQ7B)	3,000-10,000 AGL	72-97	1308	1-4 hrs.	2283
Flood Inundation Mapping	Aerosonde (MK47)	4,000 AGL	46-51	127	1-4 hrs.	177
Stream Flow Monitoring	Aerosonde (MK47)	4,000 AGL	46-51	202	1-4 hrs.	236

**Table 4: Performance Data for UAS Missions using BADA-based aircraft models**

### C. Traffic Scenarios

For this study, a NAS-wide simulation in ACES, manned VFR traffic and unmanned aircraft performing a variety of representative missions at different altitudes were simulated in ACES. The VFR traffic was collected by the 84th Radar Evaluation Squadron (RADES) at Hill AFB, Utah. The RADES collects data through the Eastern and Western Defense sectors and provides those data to a variety of government entities, including the FAA and Department of Defense. The squadron ensures that there is reliable and accurate sensor information for air traffic to support day-to-day operations, contingencies and specialized activities (e.g. counter-narcotics, search and rescue, etc.). To accomplish this, they maintain continuous real-time feeds from short-range radars in the interior of the United States and long-range air route surveillance radars that cover the perimeter. The RADES provides track updates on both cooperative and non-cooperative aircraft, however this study focuses on encounters between UAS and cooperative VFR aircraft. Future work will investigate the encounter characteristics of non-cooperative VFR aircraft. The raw radar-return data includes: time, the four-digit Mode A identifying code squawked by the aircraft, quantized pressure altitude measurements reported by the target, and range and azimuth measurements. To build tracks to use in the ACES simulation, several days of data were processed from four different months in 2012. To process the data, the raw radar measurements were fused together into a single track using a minimum-spanning tree clustering algorithm.<sup>xiii</sup> A Kalman filter was then used to smooth the tracks, and flight plan waypoints were extracted from the smoothed trajectory. The ACES platform requires each aircraft to have a departure and arrival airport, thus airports are added to the beginning and end of each VFR smoothed track to run in the simulation.

January 2012						
Su	M	Tu	W	Th	F	Sa
1	2	3	4	5	6	7
8	9	10	11	12	13	14
15	16	17	18	19	20	21
22	23	24	25	26	27	28
29	30	31				

April 2012						
Su	M	Tu	W	Th	F	Sa
1	2	3	4	5	6	7
8	9	10	11	12	13	14
15	16	17	18	19	20	21
22	23	24	25	26	27	28
29	30					

July 2012						
Su	M	Tu	W	Th	F	Sa
1	2	3	4	5	6	7
8	9	10	11	12	13	14
15	16	17	18	19	20	21
22	23	24	25	26	27	28
29	30	31				

October 2012						
Su	M	Tu	W	Th	F	Sa
	1	2	3	4	5	6
7	8	9	10	11	12	13
14	15	16	17	18	19	20
21	22	23	24	25	26	27
28	29	30	31			

Table 5: Selected days in 2012 for VFR traffic scenarios.

A select number of days were chosen across the four seasons of 2012 such that no adverse meteorological conditions were impacting the VFR traffic densities. Different days of the week and different weeks in each of the months were selected to account for variability in weekday and seasonal traffic densities. The selected days used in this simulation are shown in Table 5 in beige. To characterize the VFR traffic the number of aircraft tracks, geographic distribution of tracks, and the traffic density by altitude are given in Figure 1, Figure 2, and Figure 3.

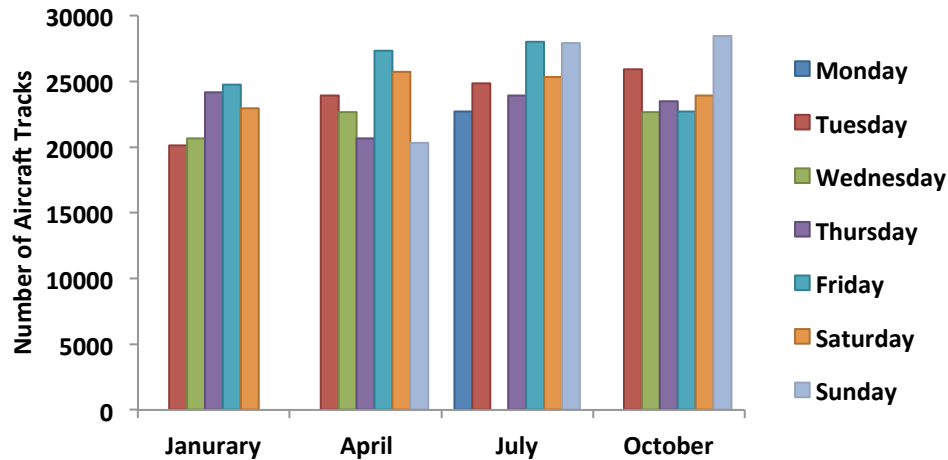


**Figure 1: Number of VFR aircraft tracks in scenario by month.**

It is evident from Figure 1, that there is no clear trend for aircraft volume by day of the week, however the summer and fall months tend to produce larger volumes than the winter and spring months. The total number of flights per day ranges from 20,000 to 28,000 and on averages is approximately 23,000.

An overlay of all VFR aircraft tracks for a single day is given in Figure 2. The radar covers most of the continental United States (CONUS), and it is clear from Figure 2 that many of the VFR flights occur around larger cities and areas of dense population.



**Figure 2: Geographic Distribution of VFR Flights for July 22nd 2012.**

Figure 3 shows the number of VFR aircraft in the CONUS by the time of day and altitude. This graphic shows that the majority of aircraft operate under 10,000 ft and between 14:00 UTC and 20:00 UTC. The UAS missions selected for this study operate at similar altitudes and times as the VFR traffic, because the DAA system is expected to provide separation primarily from VFR aircraft. The objective of this study is to understand how often these aircraft encounter each other in the absence of separation mitigations, and the nature of the encounters. This analysis will motivate the development of alerting and surveillance requirements and support the safety case for a DAA system.



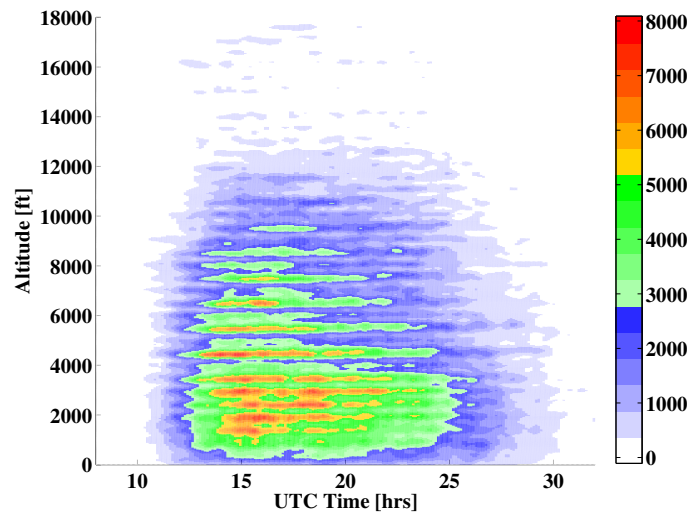


**Figure 3: Number of VFR aircraft as given by time of day and altitude level for July 25th 2012.**

#### **D. UAS Mission Descriptions**

The FAA's UAS Integration Concept of Operations<sup>XIV</sup> requires that UAS operate under instrument flight rules (IFR) and conduct operations in airspace not segregated from manned air traffic. One key challenge for UAS integration into the NAS is that the operations and flight characteristics typical of UAS differ from those of most manned IFR aircraft. While manned IFR aircraft usually fly from origin to destination airport along fixed airways and jet routes at a single cruise altitude, UAS are expected to fly "mission oriented" flight plans that can include many turns and altitude changes within a limited geographic area. The differences in flight plans between UAS and manned IFR aircraft will create different encounter rates and characteristics, so it is necessary to model expected UAS operations in order to accurately predict the safety of DAA systems that will enable UAS-NAS integration. The mission characteristics used in this study are consistent with the missions outlined in the FAA CONOPS,<sup>XIV</sup> RTCA DO-320,<sup>XV</sup> and a recent Volpe Report.<sup>XVI</sup> Intelligent Automation Inc. developed the mission sets, in collaboration with and under the supervision of NASA.<sup>XVII,XVIII</sup>

#### **Weather and Atmospheric Data Collection**

One proposed use of UAS is the collection and monitoring of atmospheric and weather data. This information is needed to evaluate and predict winds aloft so that aircraft can fly fuel-efficient routes and to feed weather forecasts on which many sectors of the economy depend. Atmospheric data collection is most accurately done today by the release of weather balloons, which is done from 91 stations across the continental U.S. The data is obtained from radiosondes that are attached to the balloons and are carried through the troposphere into the stratosphere, transmitting the collected information back to a receiving station on the ground. This data includes vertical profiles of temperature, humidity, wind speed and direction, atmospheric pressure, and geopotential height.



**Figure 4: NAS-wide UAS Atmospheric Sampling Missions, UAS tracks in white**

UAS could offer a distinct advantage in atmospheric data collection over weather balloons as they would provide a persistent observation capability and would be capable of flying to those areas in which data is most required, not simply those 91 fixed locations. A long endurance UAS would also provide round-the-clock data collection capabilities and could repeatedly climb and descend between 5,000 and 35,000 ft to sample the profile of atmospheric information.

For the mission simulated in this study, the NAS was divided into 60 grid cells and a fleet of long-endurance turbojet UAS were assigned to each cell. Each fleet provided a complete sample of the geographic and altitude-related variations in atmospheric data every four hours. The flight plans for this UAS mission are shown in Figure 4. The aircraft used to perform this mission have the performance characteristics of a Global Hawk, able to cruise at 40,000 ft and 350 kts for 24+ hours.

#### ***Cargo/Freight Operations***

UAS may be used to supplement or replace the small manned aircraft currently used in the air cargo transportation industry. Air freight delivery to small markets with light turboprop or piston aircraft is done from regional airports on an as-needed or infrequent basis. Cargo weighing less than 2000 lb is “forwarded” to one of 893 airports across the U.S., and on long flights may require either a second pilot to make the return trip or the first pilot to remain at the destination until they’ve rested for the required duration. Between 80,000 and 100,000 Cessna Caravan 208 flights carried out such cargo operations each year between 2002 and 2011. A UAS could offer lower operating costs and higher productivity than a manned cargo operation. The operating costs might be reduced because fewer personnel would be required for a given operation. Production costs could be lower than manned aircraft as some safety critical systems are no longer necessary when the pilot is not present in the cockpit (e.g., life support). Higher aircraft productivity is possible due to the absence of crew flight time limitations and the need to return crews to their operating base. These advantages of UAS cargo operations are especially evident with small planes, where there is a narrower profit margin (e.g., crew salary expenses constitute a relative large percentage of operating cost).



**Figure 5: UAS Cargo Mission Flight Profiles.**

The UAS flights selected for this mission directly replace existing light turboprop and piston cargo operations to one of the 893 airports listed as receiving small amounts of cargo in the Transportation Systems Analysis Model (TSAM) simulation tool.<sup>xix</sup> The number of daily flights is determined by the average volume of cargo received by that airport in 2012 and the relative life cycle and marginal operating costs of traditional manned cargo aircraft and a remotely piloted UAS. Nearly 500 of these flights operate each day and typically cruise between 10,000 and 18,000 ft. The origin-destination airport pairs for this mission are shown in Figure 5. The aircraft used to perform this mission have the performance characteristics of a Cessna Caravan 208, able to cruise up to 18,000 ft and 170 kts for 3+ hours.

#### ***Strategic and Tactical Wildfire Monitoring***

Manned aircraft support of wildfire fighting is currently primarily tactical: direct air tanker drops of fire retardants, transportation of personnel and equipment and some aerial observation. This support is nearly always done for existing wildfires to which firefighters are already responding, but interviews of fire professionals indicated that additional tactical observation and real-time relay of fire imagery would increase the effectiveness of firefighting operations. They also indicated that ongoing, strategic monitoring of areas with the greatest potential for wildfires would likely decrease response time to fire events and ensure the fires are smaller and easier to contain when first responders arrive. Although there is no precedent for such widespread and continuous strategic monitoring, experts believe such a capability would be justified given that it may cost more than \$1 million per day to fight a large wild land fire.

Significant expert input was used to construct the UAS missions for tactical and strategic fire fighting because of the novelty of these operations.<sup>xvii</sup> The historical record of wildfires between 2002 and 2011 was used to select operating areas for the tactical observation mission along with the airports from which the UAS would be based. To model the priority that wildfires threatening urban areas would receive for remote observation, those 17 states with OEP35 airports that constituted 90 percent of the historical wildfires were selected as the mission areas. Small airports near these mission areas were selected as UAS bases. The UAS used in this operation would be relatively small, in the Shadow-B class of aircraft, in order to balance performance and cost. Operations are conducted at 3000 ft with each mission lasting between 1 and 1.5 hours and departing at regular intervals to provide continuous coverage over the multi-day timeframe that large wildfires may take to bring under control.

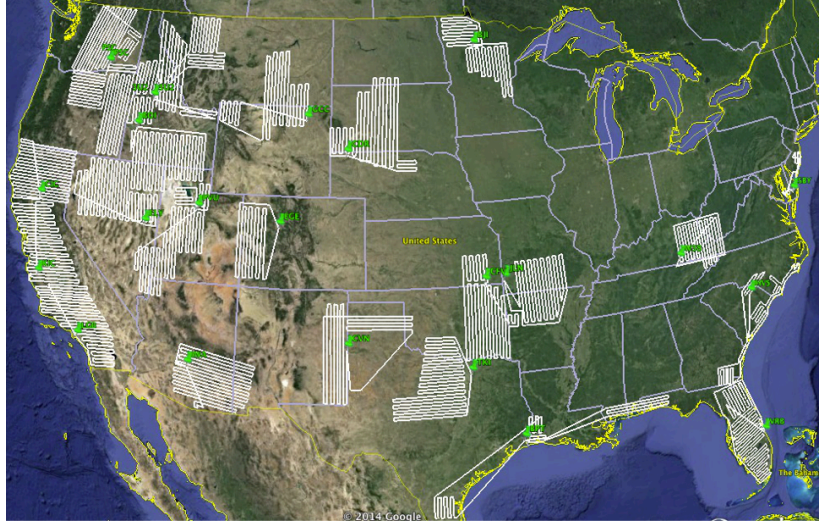


**Figure 6: Strategic wildfire monitoring mission flight plans, where the green represents the departure airport and the white lines represent the UAS flight path.**

A burn probability map developed by the Missoula Fire Science Laboratory was used to select the observation areas for the strategic wildfire detection and monitoring mission.<sup>XVII</sup> This map is based on the likelihood of wildfires occurring each year in a given area based on atmospheric conditions, local geography, extent and type of available fuel, and other factors. Twenty six missions operating out of twenty four airports were selected to cover all areas of the U.S. that are predicted to have greater than a 1% chance of burning in a wildfire each year. UAS depart on each mission with a frequency that ensures each location on the burn map is observed at least once every two hours. The aircraft cruise at 31,000 ft, an altitude that represents a compromise between larger surveillance areas available at higher altitudes and the better geographic resolution available to the infrared sensor at lower altitudes. Each flight is limited to 4400 nmi and 20 hours. These characteristics match that of NASA's Ikhana aircraft, a Predator B variant, which conducted a series of similar wildfire monitoring missions in 2007.<sup>XX</sup>

### ***Air Quality Monitoring***

Air quality standards for six common air pollutants are set by the Environmental Protection Agency (EPA), in part to preserve the health and economic well being of local communities. The degree to which these standards are met is currently evaluated through the use of fixed and mobile ground sensors, weather balloons and sondes, manned aircraft flights, and satellites. One common limitation of all of these methods is the lack of persistent data collection over time and geography. This limitation causes significant gaps in data and an incomplete account of the state of the air pollutants as air quality fluctuates throughout the day. When maturing UAS technologies reduce operating costs they may be suitable for routine air quality monitoring missions because they would offer an ability to maintain persistent surveillance at a fraction of the cost of traditional sensors. The regions with the worst air pollution and therefore the most likely to employ UAS for air quality monitoring were identified from the American Lung Association's State of the Air 2012 report.<sup>XXI</sup>





**Figure 7: UAS flight paths to monitor air quality daily in Los Angeles County, CA, where the green represents the departure airport and the white lines represent the UAS flight path.**

The air quality monitoring mission involves a UAS departing from one of 87 airports located in highly polluted regions, flying a “radiator-grill” pattern across the region between 4,000 ft. and 6,000 ft. AGL, continuously collecting pollutant data and returning to the same airport. UAS flights depart from each airport at midnight, 5 AM, 12 PM, and 6 PM local time to collect data at regular intervals. The Shadow-B (RQ7B) was the UAS modeled for this mission due to its long endurance and range, medium-sized payload capability, and its range of cruise speeds.

#### ***On-Demand Air Taxi Service***

Air taxi services in the U.S. are limited to niche markets serving small communities, islands without regularly scheduled commercial service, or executive travelers. Reduction in service to small and medium sized airports since the 2007 recession,<sup>XXII</sup> increasing hassles of flying through large commercial hubs and improvements in scheduling algorithms to match traveler demand with aircraft availability are driving increased interest in this type of service, however it remains more expensive than most comparable air carrier fares. Pilots constitute a significant fraction of overall flight operating expenses and automation may be able to play a role in decreasing costs, increasing the number of air taxi operations that occur in the U.S.



**Figure 8: On-demand air taxi service flights**

Two types of UAS-enabled air taxi services were created for this mission: a remotely piloted version that would have lower automation-conversion costs but higher per-hour operating costs, and a fully automated version that is more expensive to develop but over the long term would be less expensive to operate and therefore result in a larger number of flights.<sup>XVII</sup> Two aircraft used for air taxi operations in the past were studied for each of the automation levels, a Cessna Mustang and a Cirrus SR-22T. The number of daily flights and their origin-destination pairs were determined with TSAM by comparing expected operating costs with alternative modes of transportation. The resulting network of daily flights for the remotely piloted mission is shown in Figure 8. These SR-22T flights cruise

at 10,000 ft and 180 kts and, based on surveys of public acceptance of small aircraft and remotely piloted operations,<sup>XXII</sup> could constitute up to 7,000 flights per day in the coming decades.

### ***Flood Mapping and Stream Flow Monitoring***

Flooding takes a significant toll in terms of human and economic costs each year in the U.S., however there are no existing systematic aerial mapping programs during the course of floods or an ability to relay real-time data to responders on the ground. Only during large-scale events such as the September 2013 Colorado floods were manned aircraft used to map the extent of the inundation and measure flow characteristics using LiDAR, particle image velocimetry and sondes. Those aerial operations cost up to \$1.5 million because of the specialized instrumentation used to collect the required data. In part because of these costs and because manned aircraft were grounded due to weather, the Boulder County Emergency Operations Center contracted to fly a Falcon UAV for damage assessment for three days in the vicinity of Lyons, Colorado.<sup>XXIII</sup>



**Figure 9: Stream flow monitoring missions near Atlanta, Georgia, where the green represents the departure airport and the white lines represent the UAS flight path.**

Experts at the USGS and NOAA anticipate that UAS may eventually aid in the mapping of existing flood events, conduct damage assessment and victim location missions, collect data to improve hydrologic models and forecast flood propagation and impact. They would be employed to monitor stream-flow conditions before and after flood events, including channel depth, mean velocity, and debris contents. This type of mission followed a grid pattern along the stream direction at 4000 ft using a small UAS operated out of an airport close to the area being monitored. This altitude was selected to balance the required resolution of the sensors with a need to scan a large area. Smaller streams would need to be monitored several times per day because flow rate fluctuations can be higher than large river systems, which would typically require only one daily observation. An example stream-monitoring mission in the vicinity of Atlanta, Georgia, is shown in Figure 9. A second type of mission was flown only during flood inundation events to continuously monitor the extent of the flood impact and relay imagery to ground personnel from an altitude of 4000 ft. Both missions used a small UAS in the Aerosonde or Puma class of vehicle capable of remaining aloft for one to two hours and cruising under 50 kts.

### **E. UAS Mission Implementation**

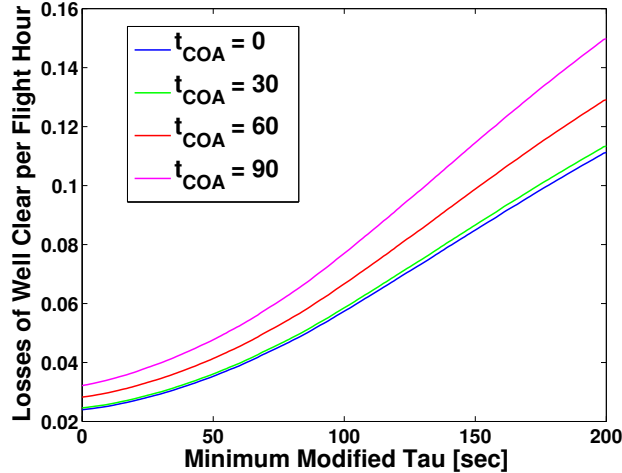
The proposed UAS missions detailed in Section D were identified by the stakeholder community and literature reviews, constructed by talking to subject matter experts, socio-economic analysis, and stakeholder input, and verified through simulation. Each mission consists of a set of flights that have altitude, speed, aircraft performance, takeoff times, duration, and geographic constraints that are dictated by that mission's requirements and objectives. This study does not include a mitigation to separate aircraft; therefore the UAS missions will come within close proximity to VFR traffic and other UAS. For this study, interactions between UAS are not analyzed and do not affect the encounter statistics. Each UAS flight is independent of the others in analysis and simulation, therefore all UAS missions were combined in a single flight data set, which was run in simulation against different days of VFR traffic. The UAS flight data set consists of the nine missions outlined in Section D, totaling approximately 18,000 flights and 26,000 flight hours over a 24-hour period.

## V. Simulation Results

### A. Analysis 1

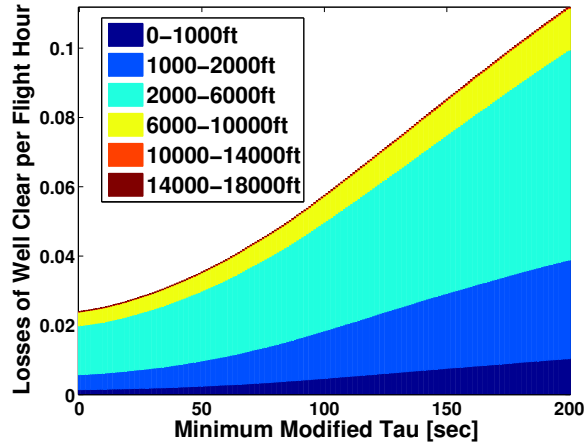
Analysis 1 evaluates the effect of parameters of the well clear definition on the rate of losses of well clear per flight hour. Definition 1 is used as a measure to evaluate the rate of losses of well clear, and each parameter variation in Table 1 represents perturbations of the baseline parameter set which is defined as D1.1. For each occurrence in which a VFR aircraft was on a converging path with a UAS and the modified tau and time to co-altitude metrics are at minima, according to the criteria of Definition 1, then the aircraft pair is recorded as an encounter. Since the simulations protocol calls for no mitigations to separate UAS and VFR aircraft, each encounter will progress until the aircraft are no longer on converging paths, which occurs at the closest point of approach.

Figure 10 depicts a cumulative distribution of encounters per flight hour as a function of the minimum modified tau for a given time to co-altitude and with the parameters of definition D1.1 (DMOD=0.80 nmi, ZTHR=600 ft, and HMD=4000 ft). This plot demonstrates the impact of setting a time to co-altitude parameter for a given tau threshold. For instance, consider a well clear definition given by the criteria in Definition 2, that has a modified tau threshold of 40 seconds, the parameters given by D1.1 and a time to co-altitude threshold of 30 seconds. Figure 10 implies that definition would yield approximately 0.033 losses of well clear per flight hour, (or 1 loss of well clear every 30.3 hours). It is evident from the contours of increasing time to co-altitude parameters that the time to co-altitude has minimal impact on encounter rate at lower values (0-30 seconds). This results from the lack of high vertical closure rate encounters between UAS and VFR aircraft to generate a protected airspace around the UAS that is sufficiently larger than the threat boundary (defined by ZTHR=600 ft, and HMD=4000 ft). Figure 10 and the subsequent plots in Analysis 1 are particularly useful in gauging the relative impact of making adjustments to the definition of well clear and the alerting criteria to inform the UAS operator of a potential loss of well clear.



**Figure 10: Cumulative distribution of encounters per flight hour as a function of minimum modified tau and time to co-altitude with well clear parameters given by D1.1 (DMOD=0.80 nmi, ZTHR=600 ft, and HMD=4000 ft).**

Figure 10 shows the aggregate statistics of all the encounters that were generated across the 20 simulated days from 2012. Taking the definition D1.1 and time to co-altitude of 30 seconds, the cumulative distribution is presented in Figure 11, where the colored regions give the relative ratio of encounters occurring at different altitude bands. Similar to Figure 10, the interpretation of Figure 11 implies that if a modified tau threshold was selected at 40 seconds an encounter would occur once every 33 hours, and of the encounters that occurred 60% would happen between 2000- 6000 ft, 25% between 1000-2000 ft, 20% between 6000-10,000 ft and 5% would occur less than 1000 ft or greater than 10,000 ft. According to this figure, the greatest contribution of encounters comes from the altitude bands between 1000 ft and 6000 ft. This is expected, as the density of VFR traffic is highest at that altitude range.



**Figure 11: Cumulative distribution of encounters per flight hour as a function of minimum modified tau and relative altitude ratio with parameters given by D1.1 (DMOD=0.80 nmi, ZTHR=600 ft, and HMD=4000 ft) and time to co-altitude of 30 seconds.**

The figures in Analysis 1 will focus on the perturbations of three parameters of the well clear definition: the horizontal miss distance, ZTHR, and DMOD. Similar to Figure 10 and Figure 11, the subsequent plots will present the cumulative plot of encounter rate per flight hour as a function of minimum modified tau. The left plot of Figure 12 shows the cumulative distribution of encounter rates as a function of minimum modified tau, where the blue line represents the D1.1 baseline condition from Table 1 (DMOD=0.80 nmi, ZTHR=600 ft, and HMD=4000 ft) where time to co-altitude threshold is 0 seconds, and the green and red lines have the same parameters as D1.1 except for an increase and decrease of ZTHR (given by condition D1.2 and D1.3 where ZTHR is 450 ft and 800 ft), respectively. The right plot in Figure 12 shows the sensitivity of the encounter rate to changes in ZTHR with respect to the baseline D1.1 condition. The sensitivity is measured by the following equation

$$\% \text{ Sensitivity to ZTHR} = 100 * \frac{\text{Encounter Rate}_x - \text{Encounter Rate}_{D1.1}}{\text{ZTHR}_x - \text{ZTHR}_{D1.1}}, \quad (14)$$

where x represents the new configuration, D1.1 is the definition from Table 1, and the parameter being changed is ZTHR. Figure 12 demonstrates that the relative impact to the encounter rates is approximately proportional to the magnitude of changes to the ZTHR parameter. For instance a 33% increase in the ZTHR parameter yielded approximately a 24% increase in the rate of encounters. This 24% increase was nearly constant for all values of modified tau. This result implies that the ZTHR parameter is minimally influenced by the time horizon and likely many of the encounters are level rather than transitioning (climbing or descending) conflicts.

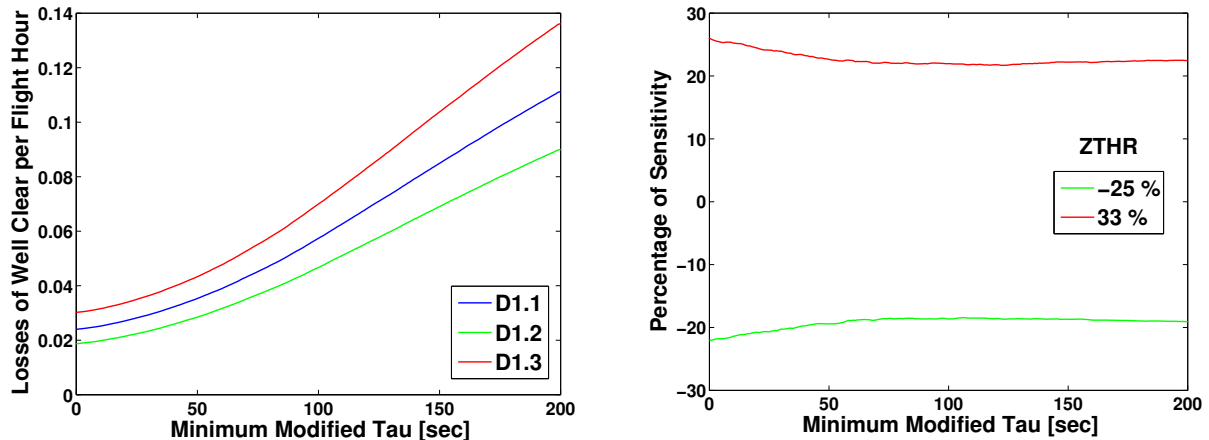


**Figure 12: Cumulative distribution of encounter rate vs minimum modified tau for different ZTHR values (Left). The sensitivity of changes to the ZTHR parameter as compared to the D1.1 definition (Right).**

Similar to the variation of ZTHR, the distance modification (DMOD) constant can be varied to investigate its impact on encounter rate. Using the same baseline definition D1.1 as in Figure 12, the cumulative distribution of encounter rates as a function of minimum modified tau with variations on DMOD are given in the left plot of Figure



13. The sensitivity to the DMOD parameter is given in right plot of Figure 13 and mimics the equation in (14) for the DMOD parameter rather than ZTHR. It is clear from the plot that there is a negligible impact from decreasing DMOD and a significant impact at smaller modified tau values from increasing DMOD. The equation given in (3) explains this phenomenon as DMOD is used as a threat boundary parameter which will set the modified tau calculation to zero when aircraft come within that parameter value. This is noticeable in the large increase in the y-intercept of Figure 13. Furthermore, it is evident from (3) that for smaller ranges the DMOD term has more influence on reducing the modified tau value. Increasing the DMOD parameter will have the greatest impact in the collision avoidance time horizon (0 to approximately 30 seconds).

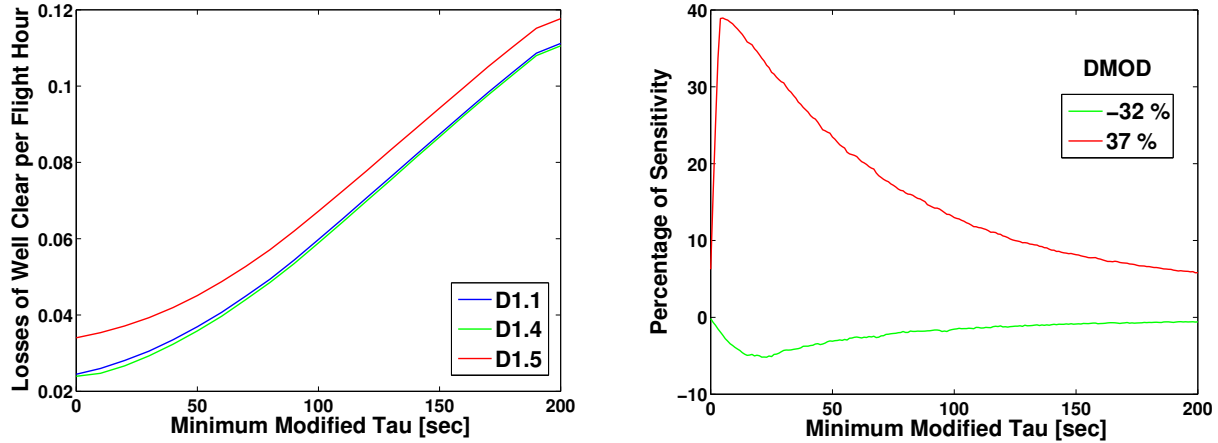


**Figure 13: Cumulative distribution of encounter rate vs. minimum modified tau for different DMOD values (Left). Sensitivity of changes to the DMOD parameter as a compared to D1.1 definition (Right).**

The variation to the horizontal miss distance (HMD) constant is given in the plots of Figure 14. The horizontal miss distance is calculated by projecting the velocity vector of the current state to a future state to determine if the range at a future state is within the HMD threshold. Similar to the variation for DMOD, a larger impact on increasing the HMD parameter as opposed to decreasing it can be observed. A decrease in the HMD parameter produces a negligible reduction in rate of losses of well clear due to using trajectory predictions based on dead reckoning and intruder aircraft that maneuver and accelerate relative to the ownship. As the HMD parameter starts to increase, the impacts are more noticeable at the smaller time horizons as the effects of the noise due to maneuvering aircraft are less pronounced.

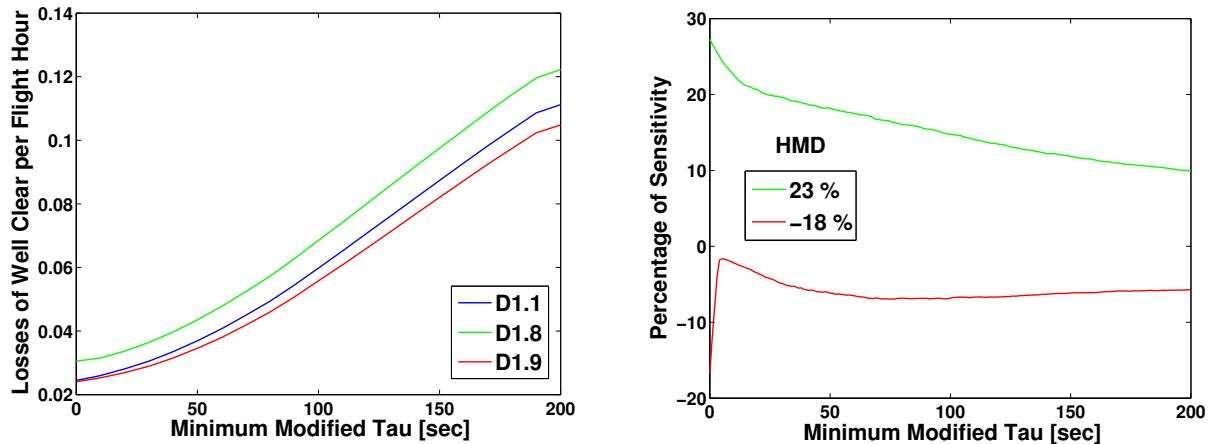


**Figure 14: Cumulative distribution of encounter rate vs. minimum modified tau for different HMD values (Left). Sensitivity of changes to the HMD parameter as a compared to D1.1 definition (Right).**

It is evident from the previous set of figures that DMOD and HMD produce similar changes in the encounter rate. From the TCAS II sensitivity level definitions, it was determined that DMOD and HMD should have the same parameter values at each of the sensitivity levels. Figure 15 demonstrates the impact of varying both the DMOD and HMD parameters. Both DMOD and HMD are set to the same value and then both parameters are increased and decreased concurrently. It is evident the encounter rates and sensitivities follow the same trend when both

parameters are increased. When the parameters are decreased, the sensitivity is larger at the small modified tau values but has a smaller impact on the rate of losses of well clear at the larger values of modified tau.

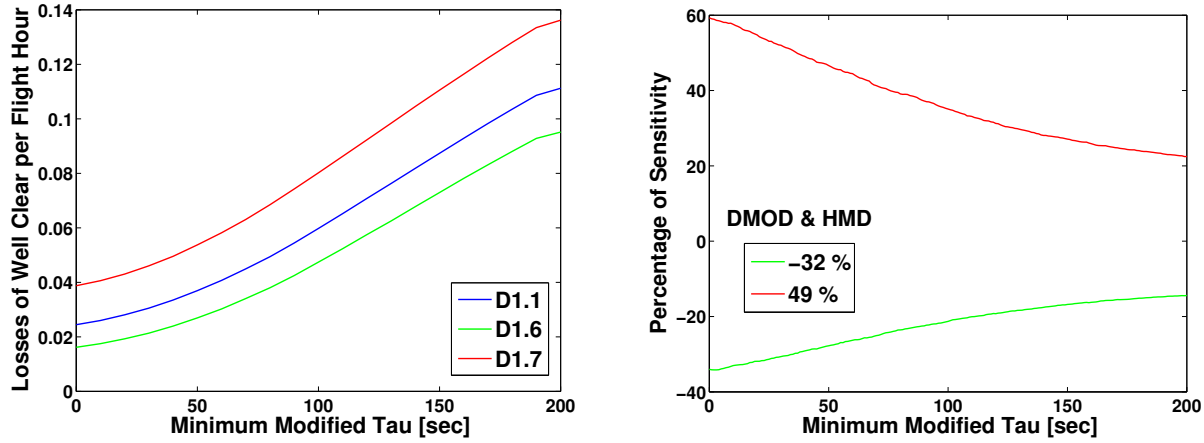


**Figure 15: Cumulative distribution of encounter rate vs. minimum modified tau for different DMOD and HMD values (Left). Sensitivity of changes to the DMOD and HMD parameter as a compared to D1.1 definition (Right).**

In summary, Analysis 1 focused on the impact of variations in the parameters of the well clear definition by comparing the sensitivity of the parameter to the rate of UAS encountering a VFR aircraft per flight hour. The rate of encounters was evaluated over a time horizon, measured by the minimum modified tau. The results from this analysis can be used to evaluate how modifications to the well clear definition. This analysis can also inform the alerting criteria needed to alert the UAS operator that action is necessary (referred to as the self separation threshold), and would influence the number of aircraft that would encounter the UAS per flight hour. The encounter rates for alerting and the well clear definition can be used in the instantiation of a safety case to evaluate the risk of collision and to inform the rate of alerting the pilot would expect due to current operations in the NAS.

## B. Analysis 2

In contrast to Analysis 1, which focused on parameter variation of a well clear definition; Analysis 2 instantiates a well clear boundary definition and investigates the relative state characteristics at the moment the boundary is crossed. This analysis will consider three definitions of well clear, two definitions were proposed by the SaRP (D2.1 and D2.2), and the third was proposed in the RTCA SC-228 Detect and Avoid Working Group (D2.3). All three definitions are based on the modified tau calculation with a horizontal miss distance at the predicted closest point of approach as detailed in equations (7)-(9).

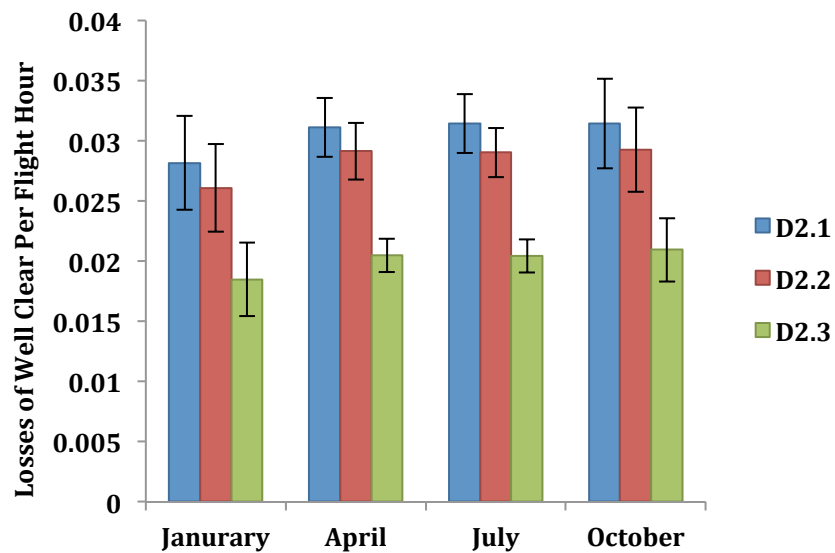
The aggregate statistics are outlined in Table 6, where it is clear that the well clear definition D2.3 yields the fewest losses of well clear. Additionally the simulation produced 270 NMAC over the 23 simulation days and yielded a probability of NMAC given a loss of well clear of approximately 1.5% and 1.6% for the D2.1 and D2.2 well clear definitions, respectively. The SaRP tuned the D2.1 and D2.2 definitions to a 1.5% unmitigated risk of NMAC given a loss of well clear using the MIT Lincoln Lab's Uncorrelated Encounter Model, and the results from the ACES simulation are consistent with the tuned unmitigated risk from the encounter model. D2.3 is based on D2.2 but decreases the ZTHR value to 450 ft, and this yields an unmitigated risk of NMAC given a loss of well clear of 2.2%.

One interoperability consideration for a well clear definition is how often an intruder's TCAS II would alert prior to a loss of well clear. The premise is that if TCAS II is alerting either the UAS operator or the intruder aircraft, then there has been a loss of well clear between the aircraft. The TCAS II alert in Table 6 is the combination of the preventative alerts and corrective alerts. From the statistics it is clear that D2.2 produces the lowest probability of a TCAS II alert, whereas D2.3 produces the highest. In today's operations, IFR and VFR aircraft are legally separated by a 500 ft altitude difference. According to the proposed well clear definitions, D2.1 and D2.3 would not register a loss of well clear if aircraft were at this 500-ft altitude separation, however D2.2 would register a loss of well clear. Table 6 demonstrates the trade-off between the operational acceptability of having a definition that is less than 500-ft in the altitude separation, denoted by ZTHR, and the interoperability and unmitigated risk of an NMAC given a loss of well clear.

	D2.1	D2.2	D2.3
Number of UAS Flight Hours	25,734	25,734	25,734
Number of Losses of Well Clear	18,139	16,867	11,938
Number of NMACs	270	270	270
Probability of NMACs given a Loss of Well Clear	1.5%	1.6%	2.2%
Probability of TCAS II RAs prior to Loss of Well Clear	4.8%	0.9%	8.6%

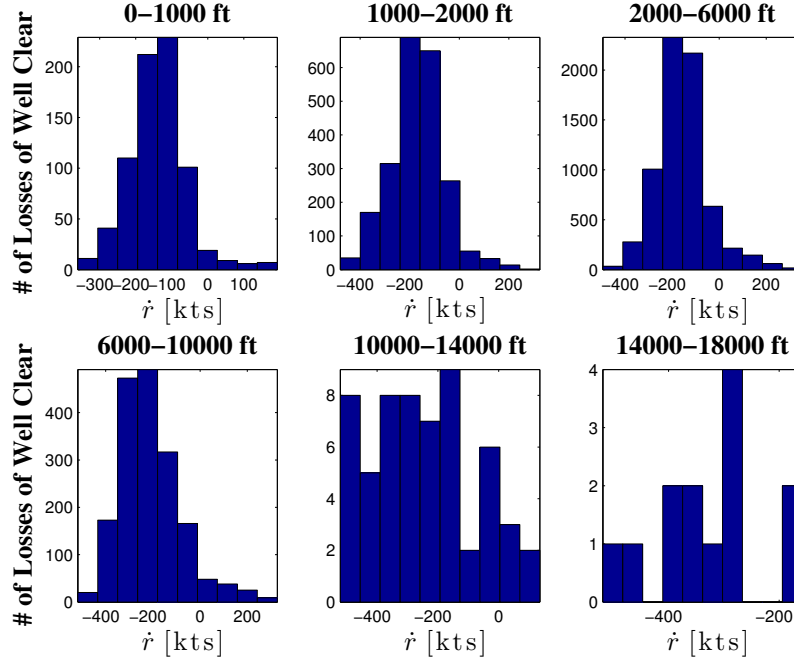
**Table 6: Aggregate statistics for well clear definitions over 23 simulated days**

Figure 16 depicts the rate of losses of well clear per flight hour grouped by the season for each of the three well clear definitions outlined in Table 2. It is clear from this bar chart that definition D2.1, which includes the time-to-co-altitude and the largest horizontal miss distance of the three definitions, has a much larger rate of losses of well clear, which is due to the larger airspace volume that is being protected by this definition. Since D2.1 and D2.2 were tuned to the same risk of collision it is expected that their rate of losses of well clear would be similar. When comparing D2.3 and D2.2 it is clear that the decrease in ZTHR to 450 ft in D2.3 has a large impact on the rate of losses of well clear (1 loss of well clear per 50 hours for D2.3 as compared to 1 loss of well clear per 40 hours for D2.2). It is also interesting to note that the seasonal effects have minimal impact on the rate of losses of well clear.



**Figure 16: Losses of well clear per flight hour for three well clear definitions (D2.1-D2.3).**

The three well clear definitions used in Analysis 2 have similarities to the alerting logic in TCAS II. The TCAS alerting logic established sensitivity levels, which vary the parameters of the definition based on altitude. These sensitivity levels were included to manage the tradeoff between necessary airspace protection and unnecessary advisories. Higher sensitivity levels, which produce larger protected airspace around each TCAS-equipped aircraft, are selected at higher altitudes to account for higher closure rates between aircraft. The well clear definitions (D2.1-D2.3) use a constant set of parameters for all altitudes. Figure 18 shows a set of histograms for the definition D2.3 at each altitude layer. It is evident from these histograms that the range of altitudes between 1,000-6,000 ft contain the highest range rates and the largest quantity of encounters. This result implies that the rate of loss of well clear is not driven by high range rates at the higher altitudes. Rather, the closure rates are comparable at the middle altitude layers, and a well clear definition might not need sensitivity levels at different altitudes.



**Figure 17: Histograms for definition D2.3 of the number of losses of well clear as a function of horizontal range rate for each altitude layer.**

Figure 18 shows a similar trend between the three definitions. The figure depicts the well clear violation rates as a function of altitude layer and demonstrates diminishing returns for protecting more airspace at higher altitudes, as the rates of losses of well clear violations are negligible.

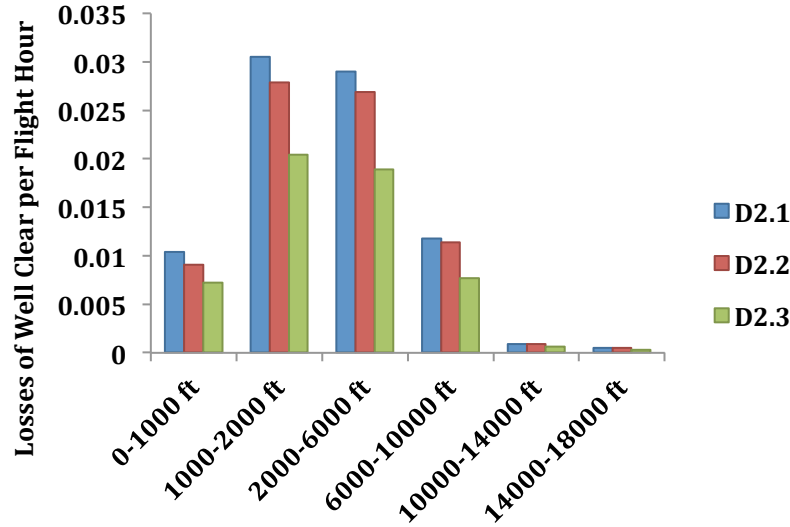


**Figure 18: Losses of well clear per flight hour for three well clear definitions (D2.1-2.3) per altitude (MSL) layer**

The relative heading between an intruder aircraft and the UAS ownship aircraft is shown for the three well clear definitions D2.1-D2.3 in Figure 19. The orientation of the plot is such that the ownship is at the origin and a head on encounter is represented by the 180 degree tick mark, whereas an overtaking encounter is represented at the 0 degree tick mark. The figure depicts 99%, 90%, 80%, and 60% contours for each of the well clear definitions. These contours represent the percentage of data contained within the contour. For instance, in the D2.1 relative heading plot, the blue line indicates that 99% of the losses of well clear are within 4 nmi of the ownship. The three well clear definitions yield similar results, as all contours are less than 4 nmi. It can be concluded that in order to avoid a loss

of well clear a DAA system would require a sensor that could see no less than 4-5 nmi in front of the aircraft. The shape of the contours implies that an intruder overtaking a UAS would yield a loss of well clear at a much closer range than an intruder and UAS in a head-on conflict. It can be concluded that the DAA system should be equipped with a sensor that can detect intruders behind the UAS at no less than 3 nmi in order to account for losses of well clear due to overtaking encounters.

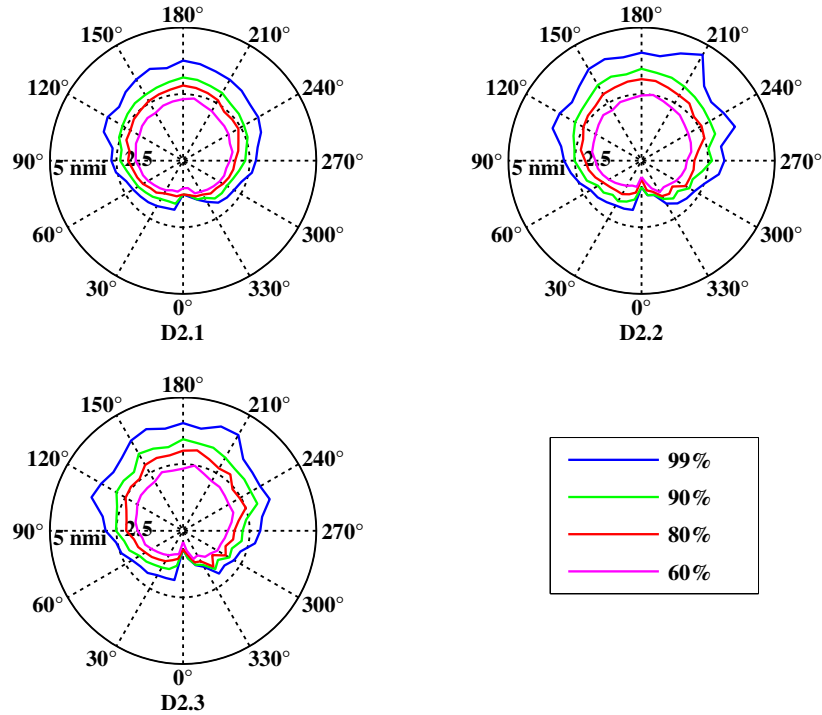


**Figure 19: Relative heading for definitions D2.1-D2.3 where contours for the boundaries are shown for the 99%, 90%, 80%, and 60% of the losses of well clear.**

The relative heading plots in Figure 19 also provide insight on the relationship between the angle at which the ownship encounters intruders and the range at which those intruders induce a loss of well clear. However, the vertical separation information is lost in this plot as all encounters are superimposed on each other. The subsequent figures will depict relationships between other parameters that define an encounter, however for brevity the plots will be shown only for definition D2.3, which is the well clear definition that has been proposed by the RTCA Special Committee 228 on Detect and Avoid Standards.

The spatial relationship between horizontal and vertical separation for a single well clear definition D2.3 is depicted in Figure 20. On the y-axis and x-axis is a histogram of the vertical and horizontal separations, respectively, at the instance of loss of well clear. The figure shows the spatial relationship between vertical and horizontal separation where the points represent separation at losses of well clear and the color corresponds to the number of losses of well clear at that spatial separation. It is evident from the figure that there are a number of losses of well clear that occur at the vertical separation boundary (450 ft) at a close proximity horizontally ( $< 1$  nmi). This is due to aircraft that are climbing or descending on the UAS ownship aircraft (or the ownship climbing or descending on an intruder aircraft) and not satisfying the vertical condition in equation (8) until they are within a close horizontal proximity from the ownship. It is also interesting to note that there is a near uniform distribution of losses of well clear at separations that are not along the vertical separation boundary (450 ft). The horizontal separation distribution is skewed towards the closer separation distances, however there is a large number of losses of well clear that occur at approximately 1.5 nmi separation from the UAS ownship. This result demonstrates the effect of the temporal separation, given by modified tau, on the amount of protected airspace. While the horizontal miss distance (approx. 0.658 nmi) is specified as the spatial boundary, given the closure rates of the intruders the modified tau criteria significantly extends the protected airspace to much larger (approx. 2 nmi) for most of the encounters.

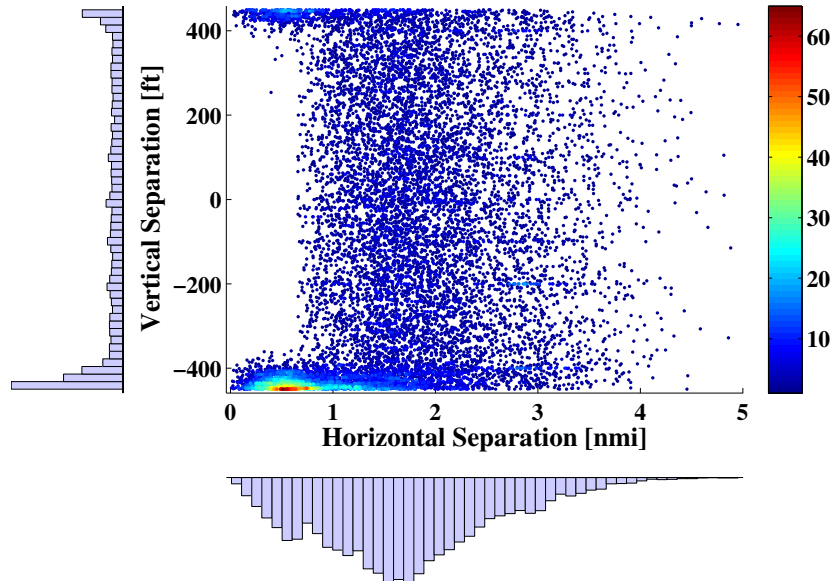


**Figure 20: Scatter plot of horizontal and vertical separation for definition D2.3 at the first loss of well clear.**

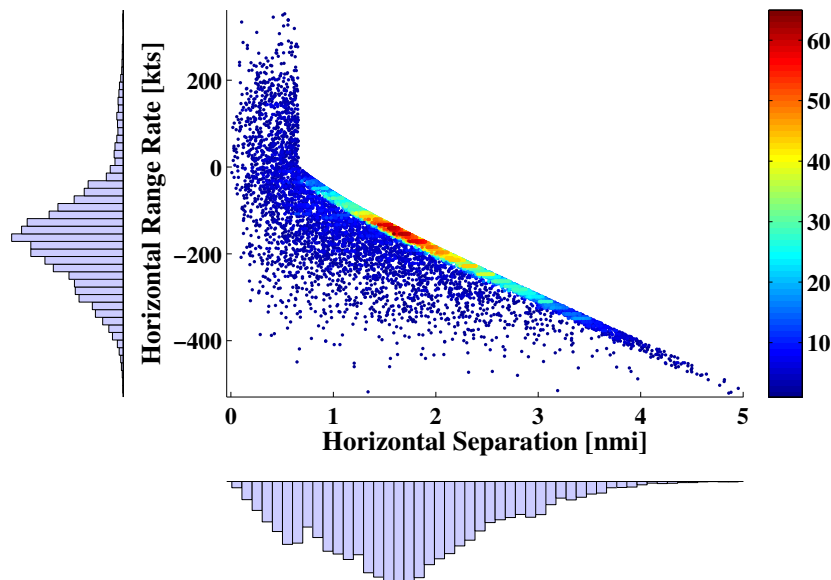


**Figure 21: Scatter plot of horizontal separation and horizontal range rates for definition D2.3 at the first loss of well clear.**

Figure 21 depicts the relationship between the horizontal range rates and the horizontal separation at the first loss of well clear for the D2.3 well clear definition. In this plot, horizontal range rate represents how timely aircraft are approaching each other, where the more negative the range rate the faster the aircraft are coming together, and a positive range rate implies the aircraft are on diverging paths. Similar to Figure 20, the histograms are provided on each of the axes and the color of the scatter plot corresponds to the density of aircraft pairs that had a loss of well clear. The scatter plot has a clear linear relationship between 0.658 nmi and 5 nmi that represents the modified tau time threshold of 35 seconds. Encounters occurring between 0.658 nmi and 5 nmi separation and under the 35-second modified tau line represent violations that happened at a modified tau less than 35 seconds. The higher the range rate the lower the modified tau value at the first loss of well clear. Points on the scatter plot that occurred closer than 0.658 nmi separation encroached on the threat boundary defined by DMOD (0.658 nmi) and ZTHR (450 ft). Specifically, a subset of the losses of well clear at the threat boundary had a positive range rate. These cases represent aircraft that were climbing or descending behind the UAS within the threat boundary. Air traffic controllers typically would consider these scenarios clear of conflict as the aircraft have already passed each other

and are on diverging paths, however given this well clear definition these cases would register to the DAA system as a loss of well clear and may request that the UAS operator initiate a collision avoidance maneuver. It is clear to see that this well clear definition could produce the most losses of well clear at 1.5-2 nmi where intruders have closure rates of 180-200 knots.

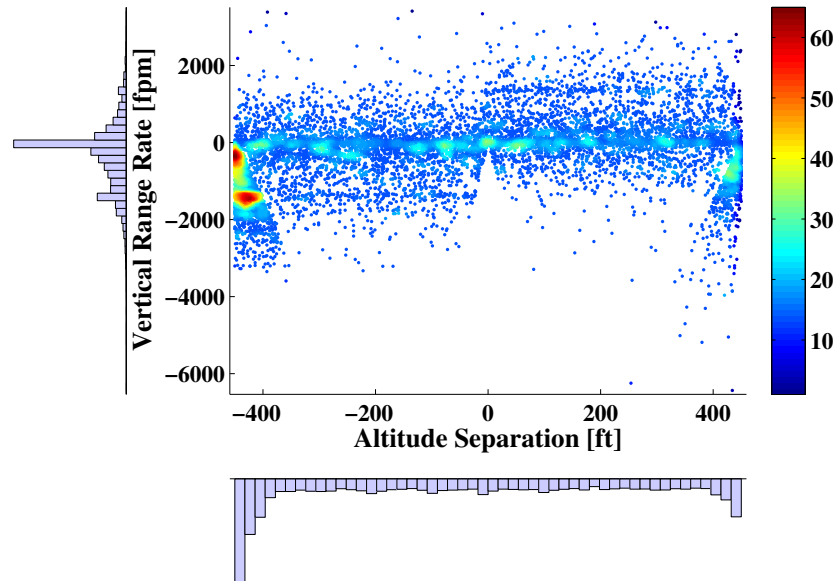


**Figure 22: Scatter plot of vertical separation and vertical range rates for definition D2.3 at first loss of well clear.**

A scatter plot of the altitude separation and vertical range rate for the D2.3 well clear definition is depicted in Figure 22, along with the histograms along each of the axes. In this plot it is evident that losses of well clear are occurring along the vertical threat boundary, denoted as ZTHR, and at a vertical range rate of zero feet per minute. This implies that a large portion of the losses of well clear occur while aircraft pairs are level with each other and vertically offset. The scatter plot also denotes a high-density area where the relative aircraft pairs are vertically converging at a rate of 1000 feet per minute and incurring a loss of well clear at the 450 ft threat boundary. These vertical closures are a relative measure and therefore could be caused from the intruder climb/descending on the ownship, the ownship climbing/descending on the intruder, or both the ownship and intruder climbing/descending into each other.

Figure 23 depicts the percentage of encounters resulting in a loss of well clear due to different types of maneuvering for definition D2.3. As expected, the majority of encounters are a result of aircraft flying straight and level on converging paths. The cases in which either the ownship is turning and the intruder is straight and level or the intruder is turning and the ownship are straight and level each constitute 5-6% of the encounters. An aircraft exceeding 3 degrees per second heading rate defines the turn in Figure 23. It is rare for a loss of well clear to occur when both the intruder and ownship are turning. There appears to be a larger percentage of transitioning encounters in which either both aircraft are climbing/descending, the ownship is climbing/descending and the intruder is straight and level, or the intruder is climbing/descending and the ownship is straight and level. There are other permutations between the ownship and the intruder, which consist of about 12-14 % of the encounters that resulted in a loss of well clear.



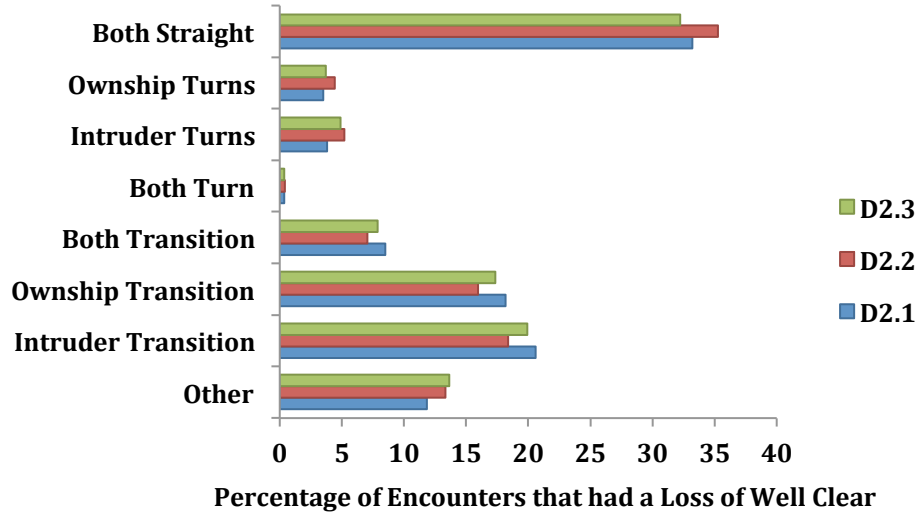


**Figure 23: Aircraft maneuvering at first loss of well clear for definition D2.3.**

In summary, Analysis 2 investigated the characteristics of encounters at the well clear boundary. This included the rate at which aircraft encroach that boundary, the relative separation, heading, and range rates, as well as the relative state of the aircraft pair. These results have implications to the safety of the well clear definition as they expose areas where the well clear boundary will be exercised based on current VFR traffic in the airspace. For comparison, three well clear definitions were presented, however for brevity, relative statistics were only presented for the D2.3 definition. It was observed that seasonal variation had limited influence on the rate of encounters, sensor ranges need to be chosen at a sufficient minimum distance as to capture most losses of well clear (3-5 nmi), the DAA system may need logic to protect against alerting the pilot to losses of well clear that occur while the aircraft are on diverging paths, and the majority of conflicts are resulting from level conflicts, however transitioning conflicts do occur in significant numbers and at moments in which aircraft are at close proximity (< 1 nmi) with each other. These results expose the need for effective alerting and vigilance by the UAS operator to maintain safety for UAS operations in the NAS.

### C. Analysis 3

Analysis 3 investigates criteria by which to alert the UAS operator that action is necessary to avoid a potential loss of well clear. This analysis considers an extension of the well clear boundary parameters for alerting, and parameters of the alerting definition will be varied. The analysis will focus on the relative state between the aircraft pairs in conflict at the first alert. In particular the range rates, relative heading and separation are of interest, as well as the percentage of alerts that did not result in a loss of well clear. While Analysis 2 assessed the safety implications of aircraft that were in a loss of separation, Analysis 3 will assess the impact to the UAS operator based on the frequency of alerts, their timeliness, and the relative state between the aircraft at the first alert. All of these have implications for the DAA sensor requirements.

The configurations used in the analysis are based on the well clear definition given by definition D2.3 and detailed in Table 3. The parameters that are varied in this analysis are: the self-separation threshold for modified tau, denoted as  $\tau_{mod}^*$ , the altitude separation threshold, denoted by ZTHR, and the minimum miss distance modification variables DMOD and HMD. Definition D3.1 uses the definition for well clear in D2.3 (modified tau of 35 seconds, DMOD of 0.658 nmi, ZTHR of 450 ft and HMD of 4000 ft) and extends the self-separation threshold (SST) to 90 seconds. This in effect is adding a buffer on the temporal dimension. Definition D3.2 extends this idea by adding a buffer to both the time threshold of 90 seconds and the altitude threshold of 700 ft. The temporal aspect of the alerting criteria is anticipated to be the most impact, therefore D3.3 and D3.4 use the definition of D3.2 and extend the self-separation threshold to 110 seconds and decrease the self-separation threshold to 70 seconds, respectively. Definition D3.5 uses the definition D3.2 and extends the minimum separation thresholds to 6000 ft HMD and 0.987 nmi DMOD. The vertical separation threshold and minimum horizontal separation threshold are increased with respect to D3.2 in the D3.6 definition. The selection of the self-separation threshold will largely be driven by the minimum sufficient time required for the UAS operator to receive an alert, gain situation awareness, determine the threat and a possible resolution, if time permits contact air traffic control and request a clearance amendment,

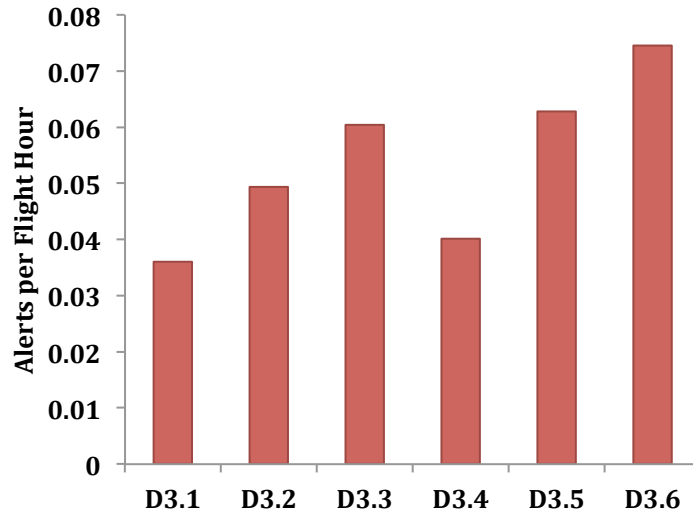


command the UAS to perform a self-separation maneuver, and for the aircraft to execute the maneuver. An excessively large SST would produce frequent alerts to the pilot and a threshold that is too small may give the pilot, an insufficient amount of time to avoid a loss of well clear. The buffers added to the minimum horizontal and vertical separation thresholds are to account for sensor, navigation, and maneuver uncertainty.

	D3.1	D3.2	D3.3	D3.4	D3.5	D3.6
<b>Number of UAS Flight Hours</b>	25,734	25,734	25,734	25,734	25,734	25,734
<b>Number of Alerts</b>	21,319	29,230	35,754	23,712	37,182	44,116
<b>Number of losses of well clear (using D2.3)</b>	11,938	11,938	11,938	11,938	11,938	11,938
<b>Number of NMACS</b>	270	270	270	270	270	270
<b>Probability of a loss of well clear given an alert</b>	55.9%	40.8%	33.3%	50.3%	32.1%	27.0%
<b>Probability of NMAC given an alert</b>	1.26%	0.92%	0.75%	1.13%	0.72%	0.61%

**Table 7: Aggregate statistics for alerting criteria over 23 simulated days**

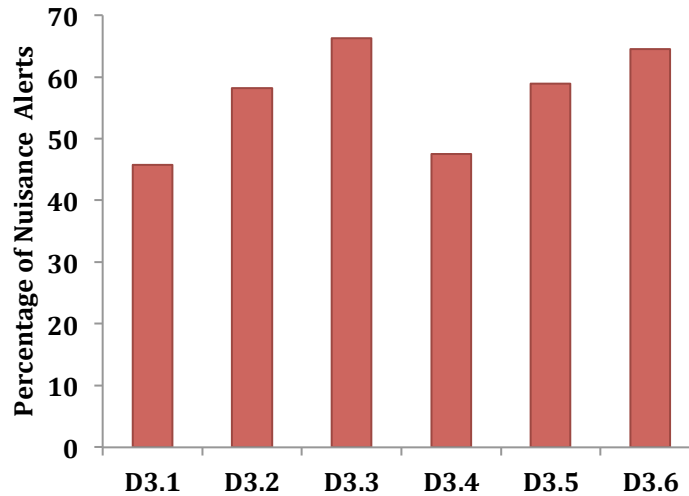
The aggregated statistics for the number of alerts over the 23 simulated days are presented in Table 7. As expected, the number of alerts scale with the size of the airspace monitored by the alerting criteria. The results show the smaller the buffered volume the larger the probability of NMAC and larger the probability of a loss of well clear. The unmitigated probability of loss of well clear given a SST alert and the probability of a NMAC given an SST alert are two metrics that are useful in the derivation of two risk ratios for the DAA safety cases. The risk ratio measures the relative effectiveness of mitigation, and the metrics presented in Table 7 form the denominator of the two risk ratios, where the numerator corresponds to the mitigated probability of loss of well clear given an SST alert and the mitigated probability of NMAC given an SST alert. The subsequent figures will explore the characteristics of the alerts and the encounters.



**Figure 24: Rate of alerts issued per flight hour**

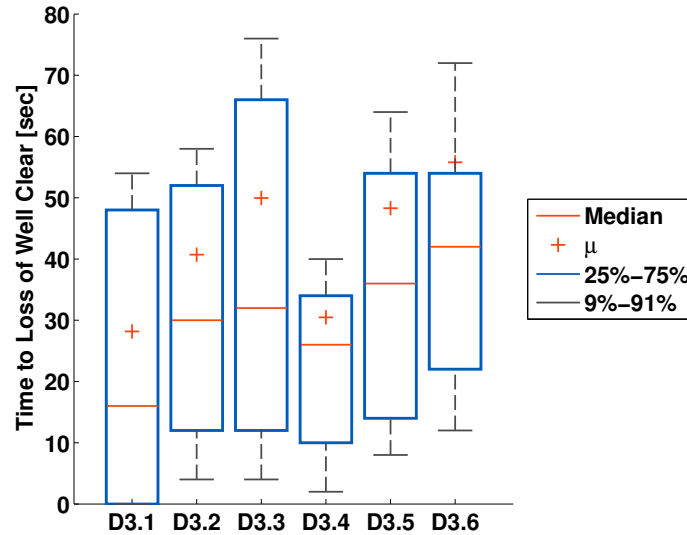
Figure 24 depicts a histogram of the rate of alerts that were issued per flight hour for each of the alerting definitions. It is interesting to note that the well clear definition D2.3 produced an unmitigated loss of well clear once every 50 hours, whereas extending just the SST for alerting produced an alert rate at once every 28 hours, as shown by D3.1. By increasing the ZTHR in D3.2, an alert was issued once every 20 hours, as shown in D3.2. Comparing D3.2 alerting rate to D3.6 it can be observed that the threat boundary defined by DMOD, ZTHR and HMD have a large effect and produces an alert once every 13 hours when all parameters were increased as given by D3.6. The alerts can be distracting to a UAS operator if they occur too frequently. In addition, if alerts that are issued are not representative of an actual potential threat to the UAS then confidence in the automation can be lost. The SST is intended to alert the pilot that action is necessary to avoid an imminent threat. Therefore, if a UAS operator consistently is alerted to proximate aircraft that are not likely to pose an imminent threat, then the operator may determine that the alerting is inaccurate and adaptive their behavior to disregard the alerts. While this alerting is not directly a safety concern it can raise the workload of the UAS operator, which could lead to a hazardous situation. In this work we define nuisance alerts as alerts that were predicted to lose well clear at a future time but ultimately would not result in a loss of well clear if no action was taken. In some contexts these alerts have also been described as false alerts with respect to the well clear definition.

Figure 25 depicts a histogram of the percentage of nuisance alerts for each of the alerting definitions. As expected the larger buffered volume for alerting yields the larger percentage of nuisance alerts. It is clear from Figure 25 that the SST is a large driver in the nuisance alert percentage. The maneuvering of either the intruder or the ownship causes these nuisance alerts, therefore a larger SST allows for a longer time horizon upon which either aircraft could maneuver. One disadvantage of the alerting logic is that both the UAS and intruder aircraft states are projected forward in time using dead reckoning, therefore if either aircraft is currently maneuvering alerts may be issued even though the aircraft have a minimal likelihood of a conflict. So while the alert is correct based on the linear state projection, the lack of knowledge of intended flight path of the UAS would cause the alert to be issued when there is no imminent collision threat present. It is expected that the percentage of nuisance alerts would be lower if the trajectory intent of UAS ownship were considered in the alerting logic.



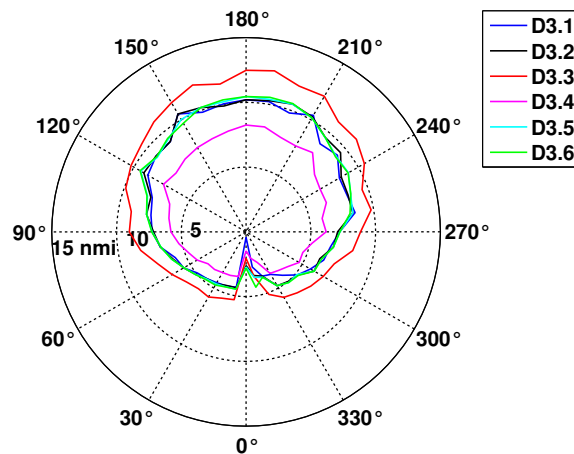
**Figure 25: Percentage of nuisance alerts issued for each of the alerting definitions.**

In addition to the frequency and reliability of alerts, it is also important that the alerting is timely enough for the pilot to perform a maneuver prior to a well clear violation. Figure 26 depicts a box-and-whiskers plot of the time until the loss of well clear. In this plot, the box represents the data between the 25<sup>th</sup> and 75<sup>th</sup> percentiles, the line inside the box represents the median, the plus symbol represents the mean and the solid black line represents the whiskers, which denote the 9<sup>th</sup> and 91<sup>st</sup> percentile values. Data outside the span of the whiskers are considered outliers and omitted from this plot. It is clear from D3.1 that when no buffers are present it is possible for aircraft to not pose a threat until after they are within 35 seconds modified tau, which is the boundary of the well clear definition. For a head-on encounter scenario, the definition D3.1 should yield a time to loss of well clear of 55 seconds, however it is clear that the mean (30 seconds) and median (17 seconds) are far below that value. This result demonstrates that due to maneuvering intruders relative to the UAS ownship, often aircraft will induce an alert at a modified tau lower than the SST. Comparing D3.1 and D3.2 depicts the impact of the vertical buffering on ZTHR, where it is evident that the mean and median of the time to well clear increases. Adding a vertical buffer appears to be a necessity, as it increases both the mean and median of the alerts above 25 seconds. Increasing the alerting time expands the range of how early alerts are issued, however it is evident from D3.2-D3.6 that the percentage of alerts issued late is a function of the size of the buffers on their vertical and horizontal minimum separation distances.



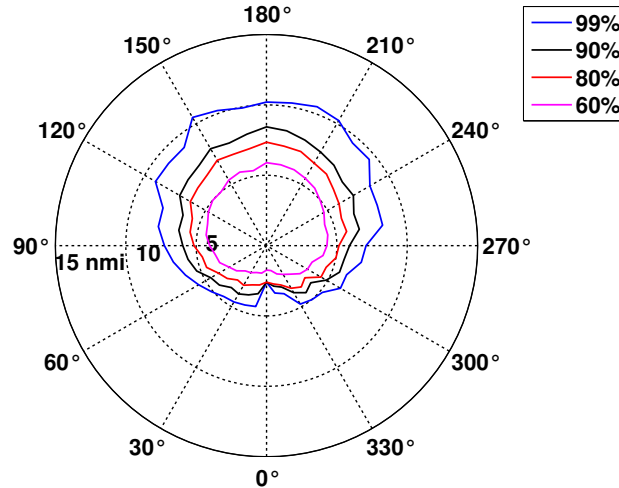
**Figure 26: Time to loss of well clear at first alert for each of the alerting definitions.**

Another important aspect of the alerting logic that has implications for the sensor requirements is the relative range between the intruder and ownship at the first alert. While Figure 19 in Analysis 2 inferred the minimum range required of the sensor to detect all intruders at the well-clear boundary, Figure 27 informs the minimum sensor requirements needed to detect an intruder for a given SST. Figure 27 depicts a relative heading plot where 99% of the data is contained within each contour for each alerting definition. In order to avoid a loss of well clear, the alerting logic needs to ensure that a UAS operator has sufficient time to detect and resolve the conflict. This result informs what surveillance range is needed to detect intruders given an SST. Future studies will consider a resolution algorithm and human-in-the-loop (HiTL) evaluation to determine whether the SST defined is sufficient to avoid a loss of well clear. Figure 27 illustrates when the SST is set to 70 seconds the sensor requirements would be 7 nmi head-on and 4 nmi in-trail, whereas if the SST is set to 110 seconds the sensor requirements are extended to 12 nmi and 6 nmi in-trail.



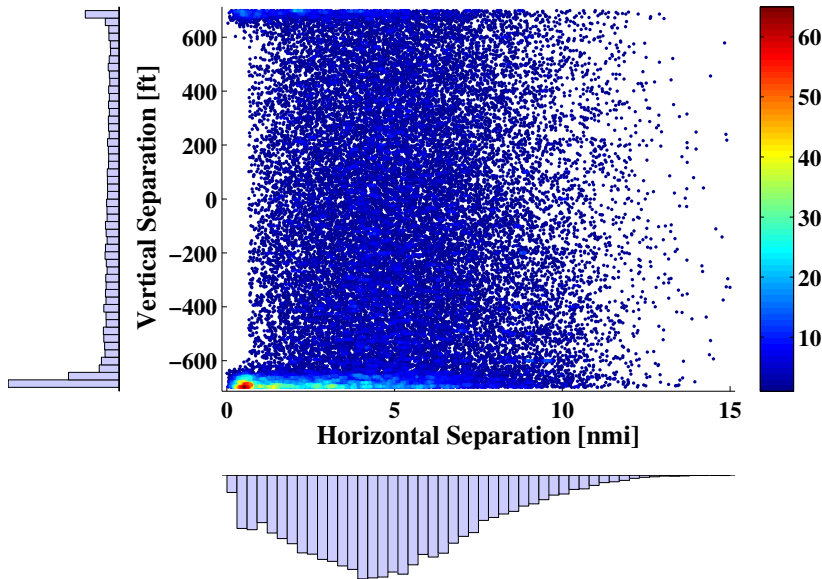
**Figure 27: Relative heading at the first alert for all alerting definitions.**

To provide more information about the characteristics of the intruder aircraft, the subsequent plots consider the D3.2 definition and depict the relative heading, spatial separation and closure rates at the time of first alert. Figure 28 depicts the relative heading, where the contours represent the boundaries within which 99%, 90%, 80%, and 60% of the alerts are contained. In developing surveillance requirements, it is feasible that the results from HiTL and fast-time simulations may yield an SST range that is acceptable for avoiding a loss of well clear, however inherently extends the surveillance range beyond the limits of current technology. In this scenario, the standards may specify an acceptable number of late alerts to ease the burden on the technology requirements. Figure 28 indicates the percentage of alerts that would still be issued from a reduced surveillance range. The alerts that would have occurred between the required surveillance range dictated by the acceptable SST and the reduced surveillance range dictated by the technology are expected to manifest themselves as late alerts due to the reduced surveillance range.



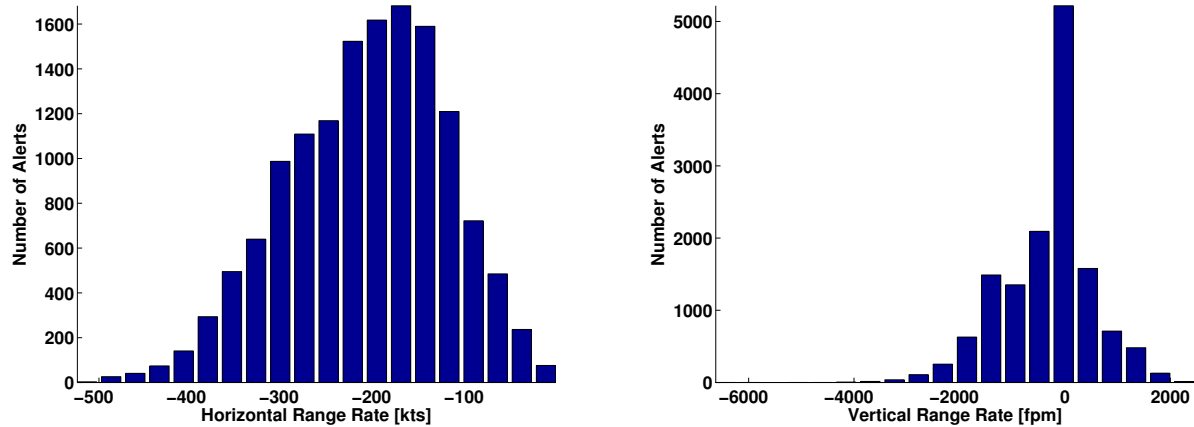
**Figure 28: Relative heading for definitions D3.2 where contours for the boundaries are shown within which 99%, 90%, 80%, and 60% of the alerts occurred.**

Figure 28 does not reflect the altitude information, as alerts at all altitude layers are super-imposed on each other to display the relative heading and range information. Figure 29 illustrates a scatter plot of the spatial relationship between the horizontal separation and vertical separation between the intruder and ownship at the instance of the alert. Similar to observations in Analysis 2 with the D2.3 well clear definition, it is evident the vertical separation is nearly uniform except at the boundary conditions. The horizontal separation tends to have more alerts between 3-7 nmi, whereas the alerts are more sparse outside those ranges.



**Figure 29: Scatter plot of horizontal and vertical separation for definition 3.2 at the first alert.**

Figure 30 depicts a histogram of the horizontal and vertical range rates at the first alert for definition D3.2. In rare cases, encounters with cooperative VFR traffic have maximum closure rates up to 500 knots. The mean horizontal range rate is -211 knots with a +/- 86 knots standard deviation, and the mean for the vertical range rate is -5 feet per minute with a standard deviation of 14 feet per minute. The typical closure rates the UAS can expect with VFR traffic is between 0-400 knots, with most of those being level encounters.



**Figure 30: Histograms of horizontal range rate (left) and vertical range rate (right) for the alerting definition D3.2.**

In summary, Analysis 3 was an initial investigation of the impact of parameters of the alerting criteria on the frequency of alerts and encounter characteristics. It was shown that the minimum horizontal and vertical separation distances had a meaningful impact on the frequency of alerting. It is evident that while adding buffer to the well clear definition for alerting is beneficial, as was shown on the increased time until loss of well clear box-and-whisker plots, making the buffers too large will produce more frequent alerts for the UAS operators and likely more nuisance alerts. Analysis 3 also presented data to inform the inferred sensor range detection requirements for a given SST, as well as inform the trade-off between sensor coverage and late alerts when there is a gap between required performance and technological state of the art for airborne surveillance.

## VI. Concluding Remarks

A UAS operation will have to comply with the regulatory see-and-avoid requirements by equipping with a DAA system. While manned aviation can rely on an onboard pilot to maintain a safe proximity or “well clear” of other aircraft based on their subjective judgment, a UAS must have a clear analytical definition to establish the minimum separation that is allowable to safely operate in the NAS. The results presented in this work are predicated on the assumption that an analytical definition of well clear is considered a separation standard between UAS and other aircraft. Three analyses were conducted using a NAS-wide fast-time simulation platform. Nine UAS missions consisting of approximately 18,000 flights were simulated against twenty-three days of historical cooperative VFR aircraft traffic. The UAS and VFR aircraft received no mitigation to avoid separation conflicts.

Analysis 1 focused on the impact on the rate of loss of well clear from varying parameters of a modified tau with horizontal miss distance well clear definition. The results demonstrated characteristic behavior of each of the definitions as well as identified the frequency of losses of separation those parameter changes would incur. For instance, for a well clear definition of modified tau threshold = 40 seconds, DMOD = 0.80 nmi, ZTHR = 600 ft, and HMD = 4000 ft and time to co-altitude = 0 seconds, a loss of well clear once every 30.3 UAS flight hours was observed, whereas increasing HMD by 23% yielded a loss of well clear once every 26 hours. The results from this analysis can be used to evaluate how modifications to the well clear definition or the alerting criteria for the UAS operator would impact the rate of losses of well clear or alerts that the UAS operator could expect to encounter. The encounter rates for alerting and the well clear definition can be used in a safety case to evaluate the unmitigated risk of collision.

Analysis 2 focused on the characteristics of encounters at the well clear definition boundary. Three different well clear definitions were considered, including the definition accepted by the RTCA Special Committee 228 DAA working group. The analysis established a minimum sensor range of 5 nmi head-on and 3 nmi in-trail required to detect losses of well clear. This analysis will inform the stakeholder organizations making operational standards as to the characteristics of the traffic that will be encountered, the unmitigated risk associated with the well clear definition, contribute to the risk ratio calculation to evaluate the performance of the DAA system, as well as expose any strengths and weaknesses of the definition itself.

Analysis 3 focused on the alerting criteria used to inform the UAS operator of an imminent loss of well clear. This analysis investigated the impact of adding buffers to parameters of a well clear definition from Analysis 2 to use for alerting. Analysis 3 informs the impact to the UAS operator based on the frequency of alerting, the timeliness of alert, and the relative state between the aircraft at the first alert, which have implications for the DAA sensor requirements. A key result from this analysis is to motivate the need for buffers on the minimum horizontal

and vertical separation in the well clear definitions, which allows alerts to get issued with more time for the UAS operator to initiate a resolution maneuver. It was also observed that the SST increases the span at which alerts are being issued, giving the pilot more time for maneuvering, but at the cost of requiring more capable sensors and the potential for more nuisance alerts. The three analysis presented help inform the safety case, requirements development, and operational environment of the DAA operational standards.

### Acknowledgements

The authors greatly appreciate the support and assistance provided by Mohamad Refai, James Snow, Chunki Park, and Seung Man Lee from NASA Ames Research Center.

### References

- <sup>I</sup> RTCA, Inc. Detect and Avoid (DAA) Whitepaper, March 2014.
- <sup>II</sup> Zeitlin, A., "Performance Tradeoffs and the Development of Standard," *Sense and Avoid in UAS: Research and Applications*, First edition, Edited by Plamen Angelov, John Wiley and Sons, Ltd., Chapter 2, 2012, pp.35-54.
- <sup>III</sup> Niedringhaus, W. P., and Lacher, A. R., "Initial Airspace Analyzer Evaluation of Impact of an Unmanned Aircraft Operating in Class A Airspace," IEEE Conference on Decision and Control, 2010.
- <sup>IV</sup> Federal Aviation Administration, "Sense and Avoid (SAA) for Unmanned Aircraft systems (UAS)," SAA Workshop Second Caucus Report, January 18, 2013.
- <sup>V</sup> Consiglio, M., Chamberlain, J., Munoz, C., and Hoffler, K., "Concept of Integration for UAS Operations in the NAS," 28th International Congress of the Aeronautical Sciences, Brisbane, Australia, 2012.
- <sup>VI</sup> Science and Research Panel (SARP) Well Clear Workshop, "Well Clear Definition Workshop Final Report," to be published by December 2014.
- <sup>VII</sup> RTCA, Inc., Minimum Operational Performance Standards (MOPS) for Traffic Alert and Collision Avoidance System II (TCAS II) version 7.1, DO-185B, June 2008.
- <sup>VIII</sup> Munoz, C., Anthony N., and Chamberlain J., "A TCAS-II Resolution Advisory Detection Algorithm." *Proceedings of the AIAA Guidance, Navigation and Control Conference*, August. 2013.
- <sup>IX</sup> Kochenderfer, M. J., et al. *Uncorrelated Encounter Model of the National Airspace System, Version 1.0*. No. PR-ATC-345. Massachusetts Inst. Of Tech. Lexington Lincoln Lab, 2008.
- <sup>X</sup> Sweet, D. S., Manikonda, V., Aronson, J. S., Roth, K., and Blake, M., "Fast-Time Simulation System for Analysis of Advanced Air Transportation Concepts," *AIAA Modeling and Simulation Technologies Conference and Exhibit*, AIAA 2002-4593, Monterey, CA, Aug. 2002.
- <sup>XI</sup> Poles, D. "Base of Aircraft Data (BADA) Aircraft Performance Modelling Report." *Eurocontrol Experimental Center* (2009).
- <sup>XII</sup> Wieland, Frederick, et al. "Modeling and Simulation for UAS in the NAS." *NASA Contract Report NASA/CRNND11AQ74C* (2012).
- <sup>XIII</sup> Park, C., Lee, H., and Musaffar, B., "Radar Data Tracking Using Minimum Spanning Tree-Based Clustering Algorithm," AIAA-2011-6825, 11th American Institute of Aeronautics and Astronautics (AIAA) Aviation Technology, Integration, and Operations (ATIO) Conference, Virginia Beach, VA, Sep. 2011.
- <sup>XIV</sup> Federal Aviation Administration, "Integration of Unmanned Aircraft Systems into the National Airspace System: Concept of Operations v2.0," Federal Aviation Administration, September 28, 2012.
- <sup>XV</sup> RTCA, Inc., "Operational Services and Environmental Definition (OSD) for Unmanned Aircraft Systems," DO-320, June 10, 2010.
- <sup>XVI</sup> Bedford, M. A. "Unmanned Aircraft System (UAS) Service Demand 2015-2035."
- <sup>XVII</sup> Ayvalasomayajula, S., Wieland, F.W., Trani, A., and Hinze, N., "Unmanned Aircraft System Demand Generation and Airspace Performance Impact Prediction," 32<sup>nd</sup> Digital Avionics Systems Conference, October 6-10, 2013.
- <sup>XVIII</sup> Ayvalasomayajula, S., Sharma, R., Wieland, F., Trani, A., Hinze, N., and Spencer, T., "UAS Demand Generation Using Subject Matter Expert Interviews and Socio-economic Analysis," submitted to 15<sup>th</sup> AIAA Aviation Technology, Integration, and Operations Conference, Dallas, TX, Jun. 22-26, 2015.
- <sup>XIX</sup> Baik, H., Trani, A.A., Hinze, N., Ashiabor, S., Seshadri, A., and Swingle, H., "Forecasting Model for Air Taxi, Commercial Airline and Automobile Demand in the United States," *Transportation Research Record*, vol. 2052, pp 9-20, 2008.
- <sup>XX</sup> Ambrosia, V.G., Wegener, S., Zajkowski, T., Sullivan, D.V., Buechel, S., Enomoto, F., Lobitz, B., Johan, S., Brass, J., and Hinkley, E., "The Ikhana Unmanned Airborne System Western States Fire Imaging Missions: from Concept to Reality," *Geocarto International*, Vol. 26, Issue 2, 2011, pp 85-101.
- <sup>XXI</sup> American Lung Association "State of the Air 2012." Accessed Feb. 20, 2013 from <http://www.stateoftheair.org/2012/assets/state-of-the-air2012.pdf>
- <sup>XXII</sup> Trani, A.A., H. Baik, N. Hinze, S. Ashiabor, H. Swingle, A. Seshadri, 2007, "Transportation Systems Analysis of the Small Aircraft Transportation Systems," Final Report to NASA Langley Research Center, Air Transportation Systems Laboratory, Blacksburg, VA.

---

<sup>xxiii</sup> Falcon UAV News, “Falcon UAV Supports Colorado Flooding until Grounded by FEMA,” posted September 14, 2013, retrieved on October 23, 2014 from <http://www.falconunmanned.com/falcon-uav-news/2013/9/14/-falcon-uav-supports-colorado-flooding-until-grounded-by-fem.html>.